Energy Conversion and Management 302 (2024) 118152

Contents lists available at ScienceDirect

Energy Conversion and Management

journal homepage: www.elsevier.com/locate/enconman

A novel model to assess the energy demand of outdoor swimming pools

Alessandro Buscemi *, Alessandro Biondi, Pietro Catrini, Stefania Guarino, Valerio Lo Brano

Department of Engineering, University of Palermo, Viale delle Scienze, Palermo, Italy

ARTICLE INFO

Keywords:
Outdoor swimming pools
Energy balance
Free surface evaporation
Wind speed modeling
Dynamic numerical simulations

ABSTRACT

In the Mediterranean region, outdoor swimming pools, despite having lower energy consumption compared to indoor pools, are nonetheless highly energy-intensive structures, offering significant opportunities for energy efficiency improvements. Although there are numerous studies in the literature, few of these works have been dedicated to estimating the energy consumption of outdoor pools while considering typical local meteorological conditions and their occupancy rates. This paper presents a novel energy balance model for outdoor pools that incorporates the latest correlations for calculating evaporation due to forced convection and sky temperature, a new phenomenological model for assessing the enhancement of evaporation as a function of occupancy rate, and an approach that takes into account atmospheric stability conditions in defining wind-related heat losses. The model successfully predicts the annual energy consumption data for outdoor Olympic swimming pools in Greece with a mean absolute percentage error of less than 12 %. Simulations of an outdoor swimming pool operating with water at 26.5 °C and in which the cover is not used present indicate a specific thermal energy consumption of about 2300 kWh/m^2. A decrease in water temperature by 1 °C and the use of a cover result in approximately 11 % and 30 % reduction in consumption, respectively.

1. Introduction

Among all types of sports facilities, swimming pools are the second most popular. They are often used for various activities, including swimming, water sports, and recreation [1]. The overall energy consumption of swimming pool sports centres includes electrical energy for lighting, ventilation and, electrical equipment as well thermal energy for heating the space, the pool, and hot water for showers [2].

In continental Europe and northern countries, the average energy consumption per square meter of water surface for indoor pools is approximately 5,200 kWh/m^2 [1]. However, a study of 41 Norwegian indoor pools revealed an average annual energy consumption of about 4,000 kWh/m^2 [3], while a similar Finnish facility was estimated to have a consumption of 2,800 kWh/m^2 [4]. Conversely, indoor pools in a Mediterranean climate zone were estimated to have an average annual consumption of 4,300 kWh/m^2 [1]. A more recent study by Mousia and Dimoudi [5] focused on the annual energy consumption of outdoor swimming pools in Greece, indicated that the average annual energy consumption for an outdoor swimming pool in Greece was approximately 2,500 kWh/m^2 without the use of a night thermal insulation cover and about 1,800 kWh/m^2 with its use.

From this initial review of the data in the literature, it can be concluded that although there is some inconsistency between the consumption values of pools in relation to their different geographical locations and outdoor pools in climates such as the Mediterranean display lower consumption values than indoor pools. Yet despite the use of passive consumption reduction systems, like night thermal-insulation covers [5], outdoor swimming pools still remain high energy-consuming facilities and offer many opportunities for the introduction of efficiency measures [6]. Therefore, a large number of research studies [7] have been presented with the aim of introducing innovative systems to make outdoor pools more efficient through the use of solar collectors [8–13], geothermal systems [10], heat pumps [14], thermal-insulation covers [15] phase change materials [16] and innovative thermal management techniques [17] and [18]. However, hardly any of these works have been devoted to analysing the annual consumption of outdoor pools in relation to the climatic conditions typical of their location thus, from a practical point of view, the dimensioning of water heating systems for outdoor swimming pools is still often based on empirical methods resulting in heating systems are often significantly overestimated or underestimated [19].

The energy demand of outdoor swimming pools is generated by various heat loss mechanisms, essentially related to the energy exchanges that take place between the pool and the atmosphere. Several studies available in the literature [13,19,20] show that over 50 % of heat

* Corresponding author.
E-mail address: alessandro.buscemi@unipa.it (A. Buscemi).

https://doi.org/10.1016/j.enconman.2024.118152
Received 19 October 2023; Received in revised form 16 January 2024; Accepted 27 January 2024
Available online 1 February 2024

Nomenclature

A_{max}	pool area per person at maximum occupancy, [m^2]
A_p	swimming pool surface area, [m^2]
C	infrared cloud amount or cloud fraction, [-]
c_p	specific heat, [$J{\cdot}kg^{-1}{\cdot}K^{-1}$]
d	zero-plane displacement, [m]
ΔH_w	latent heat of vaporization of water, [$J{\cdot}kg^{-1}$]
$\dot{E}$	rate of evaporation, [$kg{\cdot}m^{-2}{\cdot}s^{-1}$]
F_A	evaporation surface enhancement factor, [-]
F_{re}	daily pool water renewal factor, [-]
F_{sky}	sky view factor, [-]
F_u	swimming pool utilization factor, [-]
G	solar irradiance, [$W{\cdot}m^{-2}$]
$\overline{h}$	average heat transfer coefficient, [$W{\cdot}m^{-2}{\cdot}K^{-1}$]
h_M	convective mass transfer coefficient, [$m{\cdot}s^{-1}$]
H_p	depth of the swimming pool, [m]
L	length, [m]
N_{sw}	number of swimmers in the pool, [-]
p	pressure, [$N{\cdot}m^{-2}$]
P	perimeter, [m]
$\dot{Q}$	heat power, [W]
R_{Bo}	Bowen ratio, [-]
RH	relative humidity of air, [%]
s	thickness, [m]
t	time, [s]
T	temperature, [K]
SEC	annual specific energy consumptions, [$J{\cdot}m^{-2}$]
V	volume, [m^3]
v	velocity, [$m{\cdot}s^{-1}$]
z	height above ground level, [m]

Greek symbols

α	solar absorptance, [-]
β	wind shear exponent, [-]
ε	long-wave emissivity, [-]
θ	solar angle
λ	thermal conductivity, [$W{\cdot}m^{-1}{\cdot}K^{-1}$]
ρ	density, [$kg{\cdot}m^{-3}$]
σ	Stefan–Boltzmann constant, 5.67×10^{-8} [$W/m^{-2}(-\|\text{-})K^{-4}$]

Subscripts

a	air
c	cover
cl	clear sky
cond	conduction
conv	convection
e	free stream
eva	evaporation
fc	forced convection.
h	total horizontal
i	at water surface
heat	heating
nc	natural convection
p	swimming pool
rad	radiation
re	refill water
ref	reference
ro	roughness parameter in Eq. (23), [-]
ru	rural
s	saturated
set	set temperature
sun	solar
sky	sky
th	thermal
tot	total
un	unoccupied pool
ur	urban
v	water vapor
w	liquid water
wi	wind
z	zenith

Acronyms

EU	European Union
MAE	Mean Absolute Error
MAPE	Mean Absolute Percentage Error
ODE	Ordinary Differential Equation
SI	Supplementary Information
TMY	Typical Meteorological Year

losses from outdoor swimming pools are, in fact, related to the surface evaporation of water while the remaining losses are divided between those due to radiation and those due to convection. Evaporation is a complex phenomenon characterized by the simultaneous transfer of heat and mass [21] and is strongly influenced by air movements that can occur by forced or free convection [22]. The majority of the semi-empirical correlations reported in the literature to estimate evaporation at forced convection [23] are based on the John Dalton theory [24]. Among the earliest correlations of this type are those proposed by Carrier [25] (included in the ASHRAE Application Handbooks [26]) and that of Rohwer [27]. Over the years, many other empirical correlations have been proposed [23] including the one by Smith [28] which predicts lower evaporation rates than those of ASHRAE [26] and that by McMillan [29] which was confirmed by two subsequent literature studies [23,30]. The correlation of McMillan [29] was recently adopted in the model developed by Woolley et al [20] for an outdoor swimming pool. In another study, Hahne and Kübler [9] employed a model to analyse experimental data obtained from monitoring two distinct outdoor swimming pools. They tested various semi-empirical methods [27,31,32] and concluded that Richter's correlation [31] was more effective for the data obtained from one pool, while Rohwer's correlation [27] was more effective for the data obtained from the other. Moreover, Ruiz and Martinez [13] compared six different empirical correlations [26–29,31,32] using a TRNSYS [33] model that was validated with temperature data measured by them for an outdoor swimming pool and identified the Richter [31] correlation as the top performing. Lugo *et al.* [11], in a recent study where they tested the same set of empirical correlations on their experimental data, confirmed that Richter's [31] correlation was the best performing. The Richter [31] correlation was also adopted by both Zsembinszki *et al.* [16] and Li *et al.* [34] in their models that were validated using the same experimental dataset as Ruiz and Martínez [13]. The other widely used approach to predict evaporation from outdoor swimming pools is based on the analogy between heat and mass transfer [35]. This method was followed by Shah [36] to define an expression for the rate of evaporation from unoccupied swimming pools under natural convection conditions. The analogy was invoked first by Rakopoulos and Vazeos [37] and more recently by Lovell *et al.* [19] to predict thermal losses due to evaporation, both under natural and forced convection, from outdoor Olympic swimming pools.

An important factor to consider in modelling is the impact of the number of swimmers on the rate of evaporation, which can increase by

40–70 % [38] at maximum occupancy of the pool. Shah comprehensively reviewed the available literature on the subject, particularly for indoor swimming pools [39]. However, only a small number of energy balance models for outdoor pools [8] have taken the effect of pool occupancy into account (e.g. by introducing an amplifying constant of the evaporation rate of 20 %) and in all other cases these effects have been completely ignored [19].

Several approaches have been proposed in the literature to model convective heat losses of an outdoor swimming pool [8]. Firstly, several semi-empirical relationships have been proposed for forced convection over a horizontal surface, which linearly relate the convective heat transfer coefficient to the wind speed [40]. Examples of such correlations include those proposed by Jurges [41], Wattmuff [42], and the Australian Standards [43]. The reliability of these expressions were tested in the model of Molineaux *et al.* [12], which was validated with experimental data recorded at 5 outdoor pools. The Australian Standards correlation was also employed in the models of Hahne and Kübler [9], Ruiz and Martínez [13], Buonomano *et al.* [8], and Zsembinszki *et al.* [16], while that of Wattmuff was adopted in the studies of Lam and Chan [14], Buonomano *et al.* [8], Lugo *et al.* [11] and Li *et al.* [34]. A second approach to modelling convection losses, both forced and natural, is the one proposed by Rakopoulos and Vazeos [37] and by Lovell *et al.* [19], using the analogy between mass and heat flows as already mentioned above. Lastly, Woolley *et al.* [20] adopted a third approach in their energy balance model of a monitored outdoor swimming pool, which is based on the work of Bowen [44], where convective heat losses are correlated with those due to evaporation. This approach is widely accepted and considered to be one of the most robust methods in various fields, including micrometeorology, agricultural engineering, and hydrology [45].

A critical aspect to consider when using the different empirical correlations shown above to calculate evaporation and convection losses is that these were calibrated using wind speeds measured at different heights above the water surface. Therefore, depending on the height at which the wind speed values are measured in the vicinity of the pool, corrections may have to be made if these values are to be used as input for the different correlations [9]. To this end, for example, Molineaux *et al.* [12] adopted a power law to express the variation of wind speed with height [46], Rakopoulos and Vazeos [37] introduced a reduction correction factor to account for the "windbreaking" effect of buildings surrounding the pool and, more recently, Lovell *et al.* [19] used terrain multiplication factors and also considered the effect of the wind direction in their model.

Regarding radiative losses, in the energy balance models for outdoor swimming pools proposed in the literature [8], the exchange of long-wave radiation that occurs between the pool water surface and the sky was evaluated using the Stefan-Boltzmann equation. This equation includes the sky temperature, which is a function of both the dry-bulb air temperature and the emissivity of the sky [47]. The majority of empirical correlations that have been proposed over the years to evaluate the sky temperature differ in the expressions adopted to estimate the sky emissivity, under both clear and cloudy sky conditions [48]. Among the direct clear-sky emissivity correlations, there is Swinbank's [49]. This simple model, where emissivity depends only on the dry-bulb air temperature, was adopted in the swimming pool models of Rakopoulos and Vazeos [37], Zsembinszki *et al.* [16], Li *et al.* [34] and, more recently, Lugo *et al.* [11]. None of these models took into account the effect of cloud cover. A second family of empirical correlations relates clear-sky emissivity of the sky to dew-point temperature. Examples of such expressions include the one developed by Smith [28] based on the studies of Bliss [50], the one by Berdahl and Martin [51] (which is implemented in TRNSYS [33]), and the one by Walton [42]. Since Smith's approach [28] does not correct clear-sky emissivity as a function of sky cover, Berdahl and Martin [51] introduced a sky cloudiness factor for this purpose. Another alternative example of a correction function is that proposed by Clark and Allen [52] as a function of cloud cover expressed in oktas. Smith's correlation [28] was adopted by Lam and Chan [14], while that one of Berdahl and Martin [51] was implemented in both the models developed by Hahne and Kübler [9] and Ruiz and Martínez [13]. Finally the Walton correlation [53] was employed in the studies of Woolley *et al.* [20] and Lovell *et al.* [19] where a correction function of the type proposed by Clark and Allen [52] was adopted.

From what has been described, it is clear that defining an accurate energy balance model for outdoor swimming pools is not an easy exercise, as it requires modelling the complex energy interactions that occur between the pool water and the surrounding environment. Despite numerous approaches proposed in the literature to define these interactions, recently comparative studies have revealed new parameterizations that appear to be more accurate than previous ones. However, these new approaches have not yet been integrated into the energy models of outdoor pools. Regarding evaporation modelling, for example, Jodat *et al.* [54] recently compared models based on Dalton's theory and those based on analogy. They showed that models based on Dalton's theory produce acceptable results in forced convection regimes, but in mixed flow regimes, neither theory is capable of describing evaporation. In another very recent comparative study [21], several different correlations were tested for predicting water evaporation at forced convection. According to this research, the new empirical relationship proposed by Inan and Atayilmaz [55] is the one that best reproduces a set of experimental data obtained from wind tunnel tests. This expression is consistent with more recent approaches [56–58] that consider the evaporation rate at forced convection not as simply directly proportional to the difference in water vapor pressure. Concerning the modelling of long-wave radiative exchange, on other hand, in a relatively recent study [59], several widely used parameterizations were compared, using ground-based measurements collected from 71 locations distributed globally. From this interesting study, it was found that among 7 models, the sky emissivity model of Carmona *et al.* [60], which includes a multilinear regression function of the air temperature, the relative humidity and cloud fraction, was the best performing even for different climate types.

1.1. Novelties of the study

This paper presents and validates a new model for the energy balance of outdoor swimming pools, whose main objective is to assess the annual thermal energy demand of these facilities as a function of both the typical climatic conditions of their location and number of swimmers. On the one hand, this model incorporates some of the interesting aspects of previous models, such as: the possibility of calculating the solar absorption of swimming pools using the approach introduced by Wu *et al.* [61], or the aforementioned approach of modelling convective heat exchange from evaporation using the Bowen's ratio [44] (both of which had already been adopted in the model proposed by Wooley *et al.* [20])., the new proposed model also introduces a number of novelties, which are listed below: Moreover.

- the new correlation of Inan and Atayilmaz [55] is introduced for the first time in an energy balance model of outdoor swimming pools to model evaporation under forced convection conditions;
- a new phenomenological model for the enhancement of the evaporation rate as a function of the number of pool users, derived from Shah's model [62] for indoor pools, is introduced for the first time for the case of outdoor swimming pools;
- the recent correlation developed by Guo *et al.* [59]through a reparameterization of the original model by Carmona *et al.* [60] is used to calculate the sky temperature as a function of dry-bulb temperature, relative humidity and cloud cover;
- an extension of the power law model for the wind speed profile, first introduced in pool models by Molineaux *et al.* [12], which takes into account the roughness of area where the pool is located, the height of the surrounding obstacles and the effect of hourly variations in

atmospheric stability (as a function of the wind speed, solar irradiance and total sky cover).

In addition, the model also simulates the effect of using thermal-insulation cover on the energy balance of the pool water and thus on the decrease in consumption due to the reduction in evaporated water volumes. The model, numerically implemented using TRNSYS [33], is defined in such a way that all meteorological and astronomical input variables can be derived from the information normally available in a Typical Meteorological Year (TMY), which can be generated for the location of the pool using a global database such as Meteonorm [63].

The validation of the new model was based on data collected by Ruiz and Martinez [13] for a Spanish outdoor pool. The results showed that the new model is more accurate in predicting temperature variations in the pool than the best performing model to date for this experimental data set [16]. The analyses also allowed for testing two different approaches proposed in the literature by Shah [64] and Lovell *et al.* [19] to distinguish evaporation conditions for natural convection from those for forced convection. The study analysed the energy performance data of outdoor Olympic swimming pools in Greece, as presented by Mousia and Dimoudi [5], under typical climatic conditions. The new model's ability to predict the annual energy consumption of outdoor pools was tested, both with and without cover, and at different water temperatures. The numerical analysis demonstrated how varying wind exposure conditions of the pools can affect the variability of energy consumption measured in these facilities.

2. Methods and materials

In this section, the new energy model for outdoor swimming pools proposed in this work is described. To achieve this, the different expressions used to model the energy exchanges between the pool and the surrounding environment have been detailed. One subsection explains the new approach proposed to estimate the effect of pool occupancy rate on the increase in evaporation losses, while another subsection accounts for "adjusting" the wind speed profile to consider local pool conditions. Furthermore, a subsequent subsection describes the benchmark model used for validation analyses. The remaining two subsections detail the analyses defined for model validation and the case study employed to demonstrate the potential of the approach proposed in this work. However, more on the methodology is provided in the attached Supplementary Information (SI) file (Appendix A).

2.1. Energy balance model of the swimming pool

From the energy balance of an uncovered outdoor pool (see Fig. 1.a), assuming that the water is completely mixed due to filters, diffusers, and the presence of swimmers, it is possible to calculate the temporal variations of the water temperature T_w as follows [8,9,13,16,19,20,65]:

$$V_p \cdot \rho_w \cdot c_{p,w} \cdot \frac{dT_w}{dt} = \dot{Q}_{heat} + \dot{Q}_{sun} - \left(\dot{Q}_{eva} + \dot{Q}_{conv} + \dot{Q}_{rad} + \dot{Q}_{cond} + \dot{Q}_{re} \right) \quad (1)$$

where V_p is the volume of the pool, ρ_w and $c_{p,w}$ the density and specific heat of water, $\dot{Q}_{heat}$ the thermal power provided by the heating system, $\dot{Q}_{sun}$ the heat gains due to solar irradiance, while $\dot{Q}_{evap}$, $\dot{Q}_{conv}$, $\dot{Q}_{rad}$, $\dot{Q}_{cond}$, and $\dot{Q}_{re}$ correspond to the heat losses due to: evaporation, convection, radiation, conduction towards the walls and the bottom of the pool, and those associated with the volumes of water replenished daily, respectively. While conduction losses are typically neglected in the energy balance as they do not exceed 1 % [9,13,19,20] of the total heat losses, all the remaining thermal power terms appearing in Eq. (1) are discussed in detail in the subsequent sub-sections.

If, during the hours when there are no swimmers, the pool is temporarily covered to reduce evaporation losses (up to an average value of 95 % [65]), the variations in water temperature can be determined by solving the following set of coupled equations [65]:

$$\begin{cases} V_p \cdot \rho_w \cdot c_{p,w} \cdot \dfrac{dT_w}{dt} = \dot{Q}_{heat} + \dot{Q}_c - \left(\dot{Q}_{cond} + \dot{Q}_{re} \right) \\ \dot{Q}_c \simeq \dot{Q}_{sun} - \left(\dot{Q}_{conv} + \dot{Q}_{rad} \right) \end{cases} \quad (2)$$

where the first equation still represents the energy balance of the pool water volume, and the second the energy balance of the cover (see Fig. 1. b).

In the second equation, valid under the assumptions of a large surface-area-to-volume ratio and rapid energy irradiation [65], $\dot{Q}_c$ represents the power transmitted by conduction through the cover to the pool water, which can be expressed by the following relationship:

$$\dot{Q}_c = \left(\frac{\lambda_c}{s_c} \right) \cdot (T_c - T_w) \cdot A_p \quad (3)$$

where λ_c is the thermal conductivity of the cover, s_c the thickness of the cover, T_c the temperature of the external surface of the cover and A_p the surface area of the pool.

It is worth noting that the strongest assumption underlying the val-

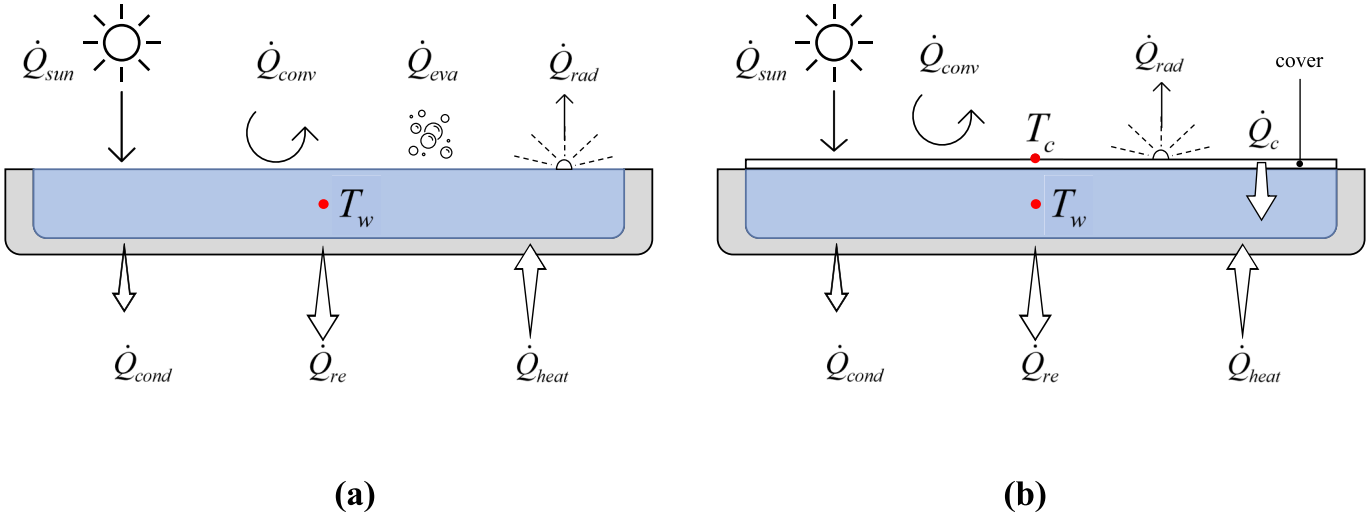

Fig. 1. Energy balance of an outdoor swimming pool: (a) uncovered; (b) covered.

idity of Eqs. 1–2 is that the temperature of the pool water is uniform due to mixing. Experimental confirmation of this assumption is provided by a recent study by Waché *et al.* [65] where the water temperature in various pools was measured at different depths. The results show that for an uncovered pool, the temperature can be assumed to be uniform both during the daytime and at night. For a covered pool, this holds true at all times when the water circulation system is active, regardless of day or night, yet during the daytime, there can be surface temperature gradients in the water just below the cover (up to a depth of approximately 10 cm) due to solar radiation when the circulation pumps are turned off. However, this situation is rare as the cover is typically used during nighttime when the pool is unoccupied and there is no influence of solar radiation. For the same reason, $\dot{Q}_{sun}$ in Eq. (2) can be considered almost always equal to zero.

2.1.1. Solar irradiance heat gains

During daylight hours, outdoor pools are exposed to solar irradiance, which contributes to providing thermal gains that can be estimated using an expression of the following form:

$$\dot{Q}_{sun} = G_h \cdot \alpha_p \cdot A_p \tag{4}$$

where G_h is the global horizontal solar irradiance and α_p the effective solar absorptance of the pool. The latter term is equal to the solar absorptance of water α_w in the case of an uncovered pool or to that of the plastic material of the cover α_c in the case of a removable blanket used to avoid water evaporation. In the case of an uncovered pool with light-colored walls and floor, several authors [8,13,14,16] have used a constant value of$\alpha_w = 0.85$ in their analyses. Hahne and Kübler [9], however, based on their theoretical analysis, showed that α_w is generally greater than 0.85 even in the case of poorly absorbing walls and floor. Despite that, from a comparison with the experimental data recorded for one of the two pools they analysed, a surprisingly low value of 0.56 for solar absorptance emerged. More recently, the study presented by Wachè *et al.* [65], conducted with a model experimentally validated using measured data from a series of 5 small outdoor swimming pools (all with a depth of 1.3 m), assessed an average value of solar absorptance equal to 0.77. The apparent inconsistency of these results is likely related to the complexity in modelling the phenomenon, as also demonstrated in the work of Wu *et al.* [61], where a methodology is presented to evaluate the solar absorptance variations of shallow water ponds based on various factors, including: the angle of incidence of solar rays θ_z, the depth of the water body, the spectral distribution of the direct and diffuse components of solar radiation and the optical H_p characteristics of the water pond floor. This approach was followed by Wooley *et al.* [20] to determine an annual average value of solar absorptance in their outdoor pool model. However, these authors did not provide any details regarding the optical properties of the walls and floor of the pool assumed in their model, nor the average value of α_w obtained from their analyses. The methodology presented in this paper follows the approach proposed by Wu *et al.* [61]. Further details can be found in SI 1.

2.1.2. Evaporative losses

Evaporation is a process in which there is a simultaneous transfer of heat and mass. This phenomenon occurs at the surface of a saturated liquid, where vapor diffuses due to molecular motion in the unsaturated gas [21]. The rate of this process is very slow when it is solely governed by molecular diffusion of the vapor. However, the process is faster when thin layers of saturated air immediately above the free water surface are removed by air currents and replaced with drier air. This air movement can occur essentially through two mechanisms: natural convection (driven by buoyancy forces) and forced convection (due to air currents, such as wind, in the case of an outdoor swimming pool) [64]. The evaporation of water in the natural convection case can be modelled through a relationship of the following type [19,35]:

$$\dot{E}_{un,nc} = h_M \cdot (\rho_{v,i} - \rho_{v,e}) \tag{5}$$

where h_M is a mass transfer coefficient for free convection, $\rho_{v,i}$ the vapor density at the water surface and $\rho_{v,e}$ the free stream vapor density. In the above and subsequent relationships, it is assumed that the air immediately above the surface of the pool is saturated with water vapor ($RH_i = 100\%$) with a temperature close to that of the water, T_w. In other words, $\rho_{v,i}$ corresponds to the saturated vapor density calculated at temperature T_w, while $\rho_{v,e}$ is the vapor density calculated considering the temperature and relative humidity of the free stream (T_a and RH_e, respectively). The expressions used to determine the coefficient h_M, as derived from the analogy of heat and mass transfer, are described in detail in SI 2. Regarding the modelling of forced convection, reference was made to a recent study [21] where ten different empirical correlations collected from the literature were compared to model laboratory-measured data. This study showed that the most effective correlation is the one proposed by Inan and Atayilmaz [55], where the vapor partial pressure difference is corrected with an exponential coefficient. This correlation, which was adopted in the model proposed with this paper, takes the following form:

$$\dot{E}_{un,fc} = (0.28 + 0.784 \cdot v_{wi}) \cdot \frac{(p_{v,i} - p_{v,e})^{0.695}}{\Delta H_w} \tag{6}$$

where v_{wi} is the wind speed, $p_{v,i}$ the vapor pressure at the water surface, $p_{v,e}$ the vapor pressure of the free stream and ΔH_w the latent heat of evaporation of water. In accordance with the assumptions described above, we have that in Eq. (6), the vapor pressure at the pool surface level can be expressed as:

$$p_{v,i} = p_{vs}(T_w) \tag{7}$$

where p_{vs} is the saturated vapour pressure (which is a function of temperature alone). Similarly, the vapour pressure of the free stream can be calculated as:

$$p_{v,e} = p_{vs}(T_a) \cdot (RH_e/100) \tag{8}$$

To define the conditions under which evaporation occurs under forced or natural convection, or a combination of both (mixed), several approaches have been proposed, including the one suggested by Shah [64], which can be described as follows:

1. If $\rho_{a,e} > \rho_{a,i}$ and $\dot{E}_{un,nc} > \dot{E}_{un,fc}$, natural and forced convection occur simultaneously, although the former is dominant over the latter: $\dot{E}_{un} = \dot{E}_{un,nc}$ calculated by Eq. (5).
2. If $\rho_{a,e} > \rho_{a,i}$ and $\dot{E}_{un,nc} < \dot{E}_{un,fc}$, natural and forced convection occur simultaneously, even though the latter is dominant over the former: $\dot{E}_{un} = \dot{E}_{un,fc}$ calculated by Eq. (6).
3. If $\rho_{a,e} \leqslant \rho_{a,i}$, evaporation can only occur through forced convection, and therefore, $\dot{E}_{un} = \dot{E}_{un,fc}$ calculated by Eq. (6).

Alternatively, Lovell *et al.* [19] utilized the following power-law relationship to model the synergistic contribution of forced and natural convection to evaporation [35]:

$$\dot{E}_{un} = \left(\dot{E}_{un,fc}^{7/2} + \dot{E}_{un,nc}^{7/2} \right)^{2/7} \tag{9}$$

with this study, as described below, the two approaches just illustrated above have been tested through the validation of the present model using the data measured by Ruiz and Martínez [13] for an outdoor pool.

The expressions for determining the evaporation rate described so far refer to the case of an unoccupied pool. In the presence of swimmers, however, the evaporation rate increases due to various physical phenomena, such as wave generation, wetted bodies of swimmers, and the generation of sprays and water droplets, all of which contribute to

increasing the effective water surface area in contact with the air [62]. Taking into consideration all these effects, it is possible to incorporate an evaporation surface enhancement factor F_A that is a function of the number of swimmers. This factor enables the calculation of the actual evaporation rate for an occupied pool using an expression of the following form:

$$\dot{E}_p = F_A \cdot \dot{E}_{un} \tag{10}$$

The correlations introduced in the literature to calculate F_A have been summarized by Shah [62] in a study where the author proposed two models, one phenomenological and one empirical. The validity of these models was tested on a limited number of experimental datasets available in the literature. All the proposed models, however, have been developed to calculate the water evaporated from occupied indoor swimming pools, aiming to both size the air conditioning systems and assess the energy consumption of the pool. For this reason, these models also consider the evaporation from the deck area wetted by splashes from the swimmers [62]. However, this last term does not need to be considered in the energy balance of an outdoor pool. Therefore, in the approach presented in this paper, a new phenomenological correlation is defined to evaluate F_A of an outdoor pool as a function of the number of swimmers, N_{sw}. The new approach, which can be derived from the original model by Shah [62] by omitting the contribution from the wetted deck, is described by the following relationship:

$$F_A(F_u) = \begin{cases} 1 + 2.3 \cdot F_u \text{ for } F_u < 0.1 \\ 1.2 + 0.3 \cdot F_u \text{ for } 0.1 \leqslant F_u \leqslant 1 \\ 1.5 \text{ for } F_u > 1 \end{cases} \tag{11}$$

where F_u is the utilization factor of the pool, defined as:

$$F_u = \frac{A_{\max}}{A_p} \cdot N_{sw} \tag{12}$$

where $A_{\max}$ is the maximum pool area per swimmer in the case of maximum occupancy, which, as indicated by Shah [62], can be assumed to be 4.5 m^2/person. In Fig. 2, a comparison is shown between the original correlation by Shah [62], validated on indoor pools (considering the contribution from the wetted deck), and the new model derived from the previous one (considering only the water evaporating from the pool) and assumed to be valid for outdoor pools.

As observed from the figure, according to the new proposed model, in the case of maximum occupancy ($F_u \geqslant 1$) of an outdoor pool, the impact of swimmers increases the evaporation rate by up to one and a half times at most compared to an unoccupied pool

Once the evaporation rate per unit of pool surface area, $\dot{E}_p$, is determined, the corresponding heat losses can be calculated using the following expression:

$$\dot{Q}_{eva} = \dot{E}_p \cdot \Delta H_w \cdot A_p \tag{13}$$

valid only if the pool is not covered.

2.1.3. Radiative losses

To quantify the net radiative heat power exchanged between the surface of an outdoor swimming pool and the environment, it is possible to use the Stefan-Boltzmann equation [8,48]:

$$\dot{Q}_{rad} = \sigma \cdot \varepsilon_p \cdot A_p \cdot F_{sky} \cdot \left(T_p^4 - T_{sky}^4 \right) \tag{14}$$

where σ is the Stefan–Boltzmann constant, ε_p the long-wave emissivity of the pool surface, F_{sky} the sky view factor, T_p the temperature of the pool surface (in K) and T_{sky} the sky temperature (in K). The pool surface temperature T_p is equal to the water temperature T_w when the pool is uncovered, and equal to the cover temperature T_c when it is covered. Similarly, the emissivity of the pool surface ε_p is equal to that of the water ε_w or that of the polymer cover ε_c in the case of an uncovered or covered pool, respectively. In this study, the long-wave emissivity of water ε_p is assumed to be 0.95, as commonly hypothesized in similar models [8,10,12,13,16].

Furthermore, the view factor F_{sky} reported in Eq. (14) is assumed to be equal to one, considering that outdoor pools have exchange surfaces with the overhead cold sky dome that are horizontal.

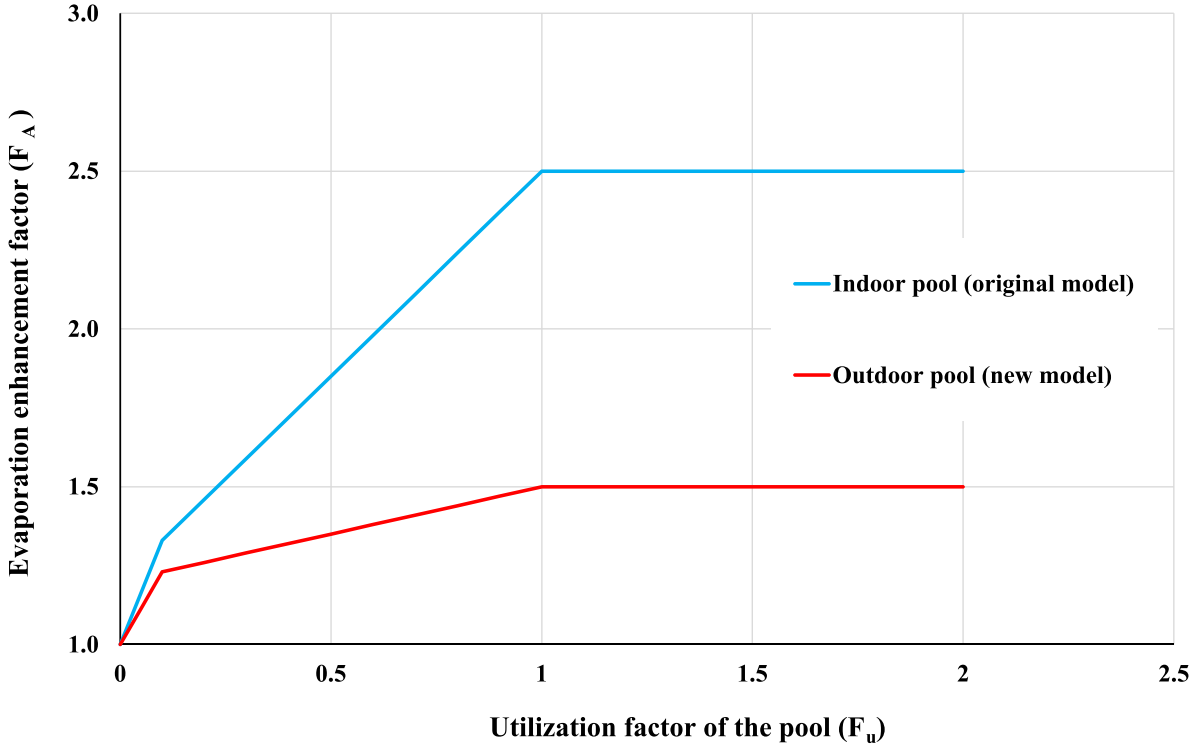

Fig. 2. Variation of F_A as a function of F_u considering the water evaporated from the wetted deck (indoor pools) and without considering it (outdoor pools).

Finally, the sky temperature T_{sky} (in K) can be related to the ambient temperature T_a (in K) through the following relationship [47,48]:

$$T_{sky} = \varepsilon_{sky}^{0.25} \cdot T_a \tag{15}$$

where ε_{sky} is the emissivity of the sky. As already mentioned in the introduction, over time, numerous empirical models have been proposed to model the emissivity of the sky [47,48,59,60]. In this study, this quantity is calculated using the expression proposed earlier by Martin and Berdhal [66], and subsequently by Crawford and Duchon [67] and Carmona *et al.* [60]:

$$\varepsilon_{sky} = \varepsilon_{sky,cl} \cdot (1 - C) + C \tag{16}$$

where $\varepsilon_{sky,cl}$ is the clear-sky emissivity and C is named "the infrared cloud amount" by Martin and Berdhal [66] and the "cloud fraction" by Crawford and Duchon [67] and Carmona *et al.* [60].

In this study, the following expression elaborated by Guo *et al.* [59] through a reparameterization of the original model by Carmona *et al.* [60], is adopted to model the clear-sky emissivity:

$$\varepsilon_{sky,cl} = -0.4373 + 0.0037 \cdot T_a + 0.0027 \cdot RH_e \tag{17}$$

where T_a is in K and RH_e in %. Guo *et al.* [59], by comparing seven different models using ground-based measurements collected from 71 locations distributed worldwide, demonstrated that the multilinear regression function of air temperature and relative humidity described by Eq. (17) performed best for various climate types. It is noteworthy to underline that through this study, the correlation of Carmona *et al.* [60] is, for the first time, used to estimate the radiative losses (under clear sky conditions) of an outdoor pool.

Finally, regarding the method used to calculate the cloud fraction C in this paper, refer to what is described in detail in SI 3.

2.1.4. Convective losses

The determination of convective heat exchange between an outdoor swimming pool and the environment was, once again, distinguished by considering both the cases of an uncovered pool and a pool covered with an anti-evaporation sheet. Regarding the first case, in this study, we chose to adopt the Bowen approach, which, as mentioned in the introduction, is considered one of the most robust methods for determining convective heat losses based on radiative losses [45]. This method, successfully applied by Woolley *et al.* [20] to model temperature variations in an outdoor swimming pool, predicts that convective heat losses, both natural and forced, can be expressed by the following relationship:

$$\dot{Q}_{conv} = R_{Bo} \cdot \dot{Q}_{eva} \tag{18}$$

where the Bowen ratio R_{Bo} [44] is defined as:

$$R_{Bo} = \left(\frac{c_{pa,e} \cdot p_{a,tot}}{0.622 \cdot \Delta H_w} \right) \cdot \left(\frac{T_w - T_a}{p_{v,i} - p_{v,e}} \right) \tag{19}$$

where $c_{pa,e}$ is the specific heat of air at T_a. Regarding the case of a night covered swimming pool, convective heat losses can be defined as a function of the temperature difference between the cover and the air using the following relationship [65]:

$$\dot{Q}_{conv} = \overline{h}_{conv} \cdot A_p \cdot (T_c - T_a) \tag{20}$$

where $\overline{h}_{conv}$ is the average convective heat transfer coefficient. Finally, for the determination of the latter coefficient, please refer to what is described in detail in SI 4.

2.1.5. Water refill losses

Several factors contribute daily to the reduction of water volume in the pool, including evaporation, the presence of swimmers, and filter backwashing. Additionally, for hygiene and sanitary reasons, especially in public pools, it is mandatory to renew a certain quantity of pool water daily. This percentage of renewal typically varies between 2.5 % and 5 % of the total pool water volume, depending on the regulations in different countries [7,8]. The replenishment water is usually drawn from the public water supply at a lower temperature than that of the pool. Under these assumptions, the thermal losses due to water renewal in a swimming pool can be estimated through a relationship of the following type [7]:

$$\dot{Q}_{re} = \left(\frac{V_p \cdot F_{re}}{86400} \right) \cdot c_{pw} \cdot (T_w - T_{re}) \tag{21}$$

where F_{re} is the daily water renewal percentage, c_{pw} the specific heat of the water and T_{re} the temperature of the make-up water coming from the aqueduct. This temperature typically varies throughout the months of the year.

2.1.6. Heating power

The conventional heating systems for pools include electric and oil/gas heaters [6]. For example, in the case of outdoor Olympic-sized pools in Greece, the majority of heating systems use both fuel oil and natural gas boilers [5]. The hydronic heating system for a swimming pool must include: a circulation pump, a water-to-water heat exchanger of the boiler, and a system of filters. The water pumped from the pool undergoes heating through the heat exchanger, until it reaches the predetermined set temperature, T_{set}, and then it is filtered before being reintroduced into the pool through the appropriate diffusers [6]. The term, $\dot{Q}_{heat}$, appearing in Eqs. 1–2, represents precisely the heat that needs to be transferred to the water by the heat exchanger to maintain the water temperature close to T_{set} during the heating designated periods. The time integration of the thermal power required to maintain T_w equal to T_{set} allows, as shown subsequently, the computation of the annual thermal demand of an outdoor swimming pool. Moreover, the adoption of dynamic energy models, such as the one presented in this study, can facilitate the identification of the thermal peak power and, thus, the sizing of the heater [19].

2.2. Wind speed adjustment

As previously highlighted, both evaporative and convective losses under forced convection are strongly dependent on the wind speed values near the water surface of an outdoor pool. With regard to this, it is worth noting that, on the one hand, numerous forced convection correlations have been calibrated using wind speed measurements taken at heights ranging from 0.3 to 2 m above the water surface [9]. On the other hand, the wind speeds typically available are measured at weather stations by anemometers located at a height typically equal to 10 m [12]. Furthermore, it is necessary to add that wind speed profiles are often locally altered by the presence of obstacles near the pool, such as buildings, vegetation, etc [37].

To account for the variations in wind speed at different heights above the ground, Molineaux *et al.* [12] incorporated a power law equation into their model for outdoor swimming pools. The power-law wind speed profile, is empirically based but widely adopted by various authors [68,69] as an alternative to the log-law model, which instead has a more rigorous physical foundation [70]. As illustrated by Irwin [71], the exponent of the power law is primarily a function of surface roughness and atmospheric stability conditions. For example, Touma [46] demonstrated how this exponent can be correlated with the Pasquill atmospheric stability class [72], considering smooth terrains typical found in rural areas. More recent studies have shown the applicability of the Pasquill stability class in defining the wind speed profile even in urban environments [69].

Based on the above considerations, in the model presented in this paper, the wind speed v_{wi} at a generic height z above the ground can be

estimated using the following expression [73]:

$$v_{wi} = v_{wi,ref} \cdot \left(\frac{z-d}{z_{ref}}\right)^{\beta} \quad (22)$$

where $v_{wi,ref}$ is the wind velocity measured at a reference height z_{ref}, d the so called zero-plane displacement and β the power-law exponent. The d parameter, as shown in Fig. 3, takes into account the modifications of the undisturbed wind profile due to the presence of obstacles in the surroundings of the pool.

In the case of the presence of obstacles ($d > 0$), the proposed model will predict that:

1. the reference wind velocity $v_{wi,ref}$, measured at z_{ref} in an area without obstacles (point A in Fig. 3) would occur at a higher elevation ($z_{ref} + d$) near the swimming pool (point A' in Fig. 3);
2. the wind velocity value computed at the height at which the forced convection correlation, for example Eq. (6), has been calibrated, exhibits a reduced value (point B' in Fig. 3) in the vicinity of the pool compared to that which would be observed in an obstacle-free area (point B in Fig. 3).

As previously described, the exponent β of the power-law of Eq. (22) is dependent on both the terrain roughness and atmospheric stability conditions. In this model, it is assumed that β can be interpolated between the value associated with a smooth surface β_{ru} (rural areas) and the value associated with a rough surface β_{ur} (urban areas) using the following relationship:

$$\beta = \beta_{ru} + (\beta_{ur} - \beta_{ru}) \cdot ro \quad (23)$$

where ro is a parameter ranging from zero to one, representing the average surface roughness of the area ($ro = 0$ for smooth surfaces and $ro = 1$ for rough surfaces). To define the two wind shear exponents in Eq. (23), refer to the tables summarised in SI 5.

As emphasized by Hahne and Kübler [9] in their investigation of two outdoor pools in Germany, the issue of accurately determining 'characteristic' wind speed values to be used as input in models for estimating evaporation losses from an outdoor pool is a practical challenge that cannot be effectively resolved with reasonable effort. Therefore, both Molineaux *et al.* [12] and Hahne and Kübler [9] preferred to treat the coefficients of the empirical correlations for convective and evaporative losses as free parameters. These parameters were adjusted to minimize errors between measured and simulated water temperature values for each pool examined.

The approach proposed in this study, on the other hand, considers the option of solely altering the parameters of the wind speed profile expression, potentially treating them as free variables of the swimming pool model. Thus, the value of z in Eq. (22) is fixed at the height above the ground for which the correlation that models forced convection evaporation is valid. As for the other two parameters, ro and d in Eqs. 22–23, they can be estimated based on reasonable assumptions or one can follow either of the following two alternative procedures for their determination:

1. in the case where the wind speed near the pool has been measured at a specific height for a sufficient period of time, the values of ro and d can be found as those that minimize the error between the measured and calculated wind speed values;

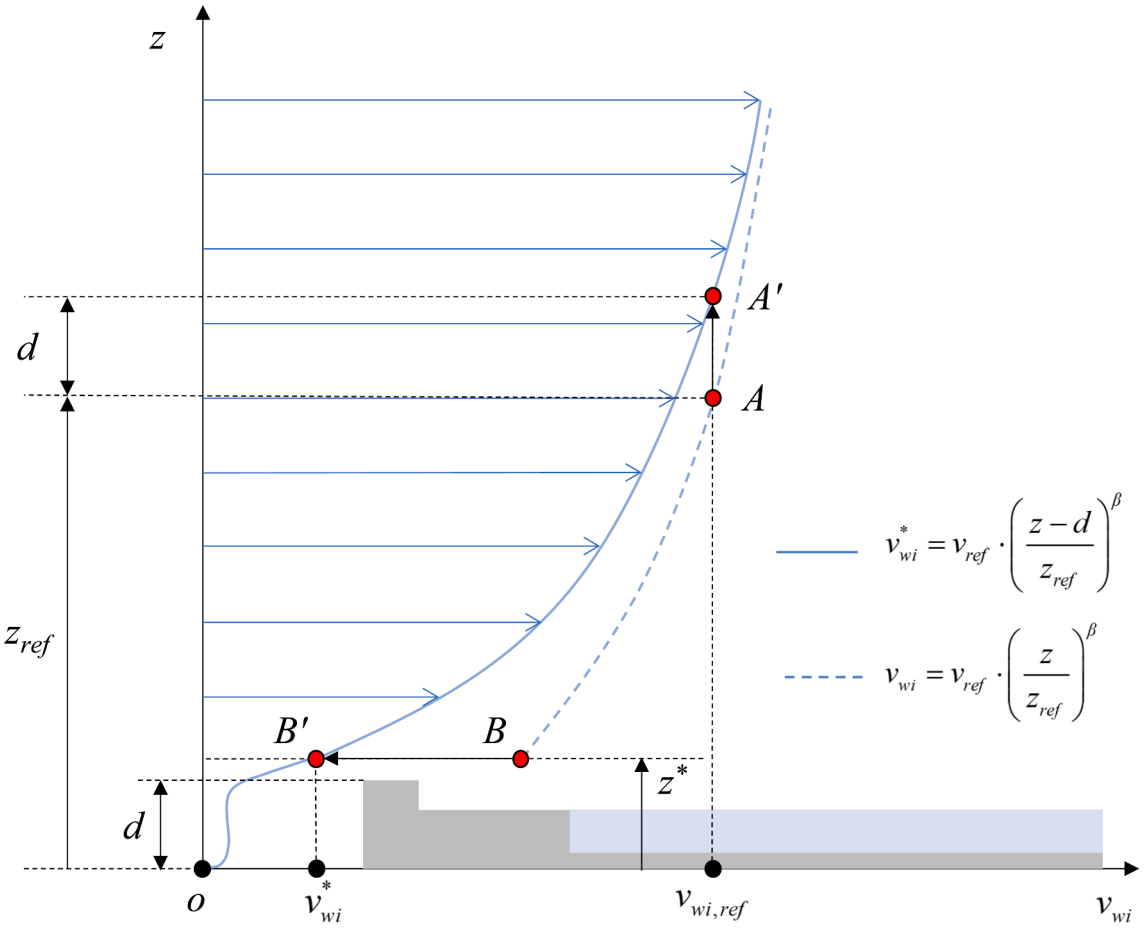

Fig. 3. Power-law wind velocity profile in the presence of an obstacle near the swimming pool.

2. in all other cases where the wind velocity is not measured locally but rather the water temperature of the swimming pool is measured or the energy consumption for its heating is known over a sufficiently long time interval, *ro* and *d* can be treated as free parameters in the energy balance model. Their values can be estimated by identifying those that minimize the error either between the measured and modelled water temperature or between the measured and modelled energy consumption.

In all the cases considered above, to calculate the variations of the wind speed profile using the proposed approach, it is necessary to determine the time series of G_h, v_{ref}, and v_{ref}. These can be defined based on the data measured from the nearest meteorological station to the pool or, depending on the analysed cases, using climatic data from a TMY generated for the geographical area of the swimming pool.

2.3. Benchmark model for validation

As described subsequently, the energy balance model for outdoor pools proposed in this study has been tested using experimental data published by Ruiz and Martínez [13] for an open-air swimming pool in Spain. To this end, the same model was benchmarked against the one proposed by Zsembinszki *et al.* [16], which was selected because it was the most accurate in reproducing the measured temperature variations for this Spanish swimming pool [13,16,34]. A detailed description of the equations that constitute this model can be found in SI 6.

2.4. Numerical implementation of the model

In this work, the proposed model, along with the benchmark model, have been implemented using the commercial software TRNSYS [33]. This software environment allows the integration of various components (known as Types) to build complex systems whose non-linear transient behaviour can be simulated. Fig. 4 illustrates the various types and macros used to construct the TRNSYS layout implementing the open-air swimming pool model proposed in this article. A detailed description of the types and macros that make up the layout depicted in Fig. 4 can be found in SI 7.

In summary, the above described TRNSYS energy balance model enables the simulation of water temperature variations in an outdoor pool based on changes in the local climatic conditions. The model accounts for both the impact of occupants on heat losses due to evaporation (during pool opening hours) and the mitigation of such losses through the use of a nighttime covering. The model's outputs encompass all energy exchanges between the pool and the surrounding environment. By integrating the heating thermal power over time, it becomes possible to calculate the annual energy consumption of the pool, considering the actual heating system operation periods, occupancy schedules, facility closure days, and more.

2.5. Validation of the model and case study

The next two subsections describe the methods used to validate a simplified version of the proposed model using experimental data from a Spanish outdoor swimming pool, and the numerical analyses carried out with the full model to study the annual consumption of Greek Olympic swimming pools in the Athens area, comparing them with data obtained from energy audits of these facilities.

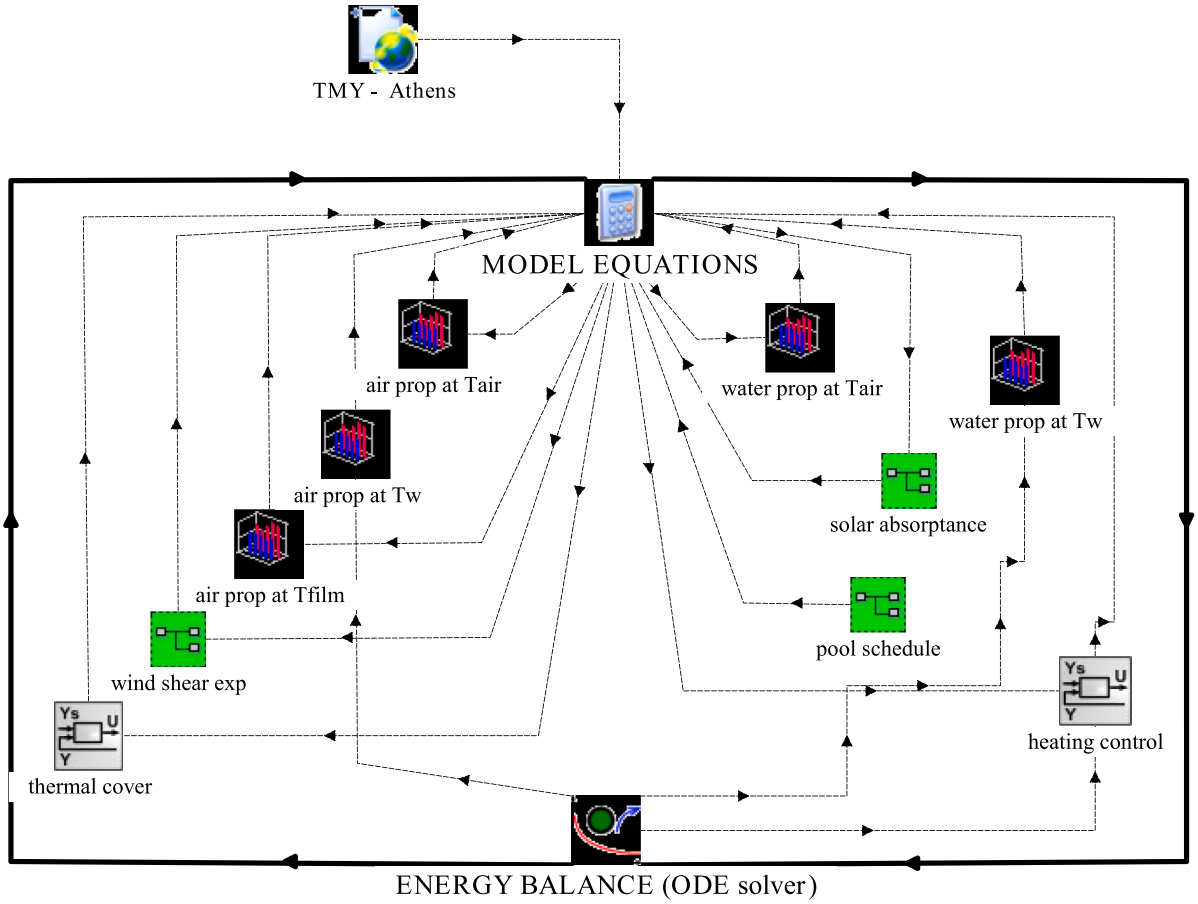

Fig. 4. TRNSYS layout of energy balance model for outdoor swimming pools.

2.5.1. Validation of the model using experimental data

As already mentioned, experimental data measured by Ruiz and Martínez [13] for a private outdoor pool (with a surface area of 50 m^2 and a volume of 82.5 m^3), located near Alicante, Spain, were used to validate the new model. This dataset was chosen because it is one of the few available in the literature for testing numerical models defined to simulate the energy balance of outdoor swimming pools. For this pool, in fact, which is not equipped with a heating system, meteorological variables (wind speed v_{wi}, air temperature T_a, relative humidity RH_e, and horizontal solar irradiance G_h) as well as the pool water temperature T_w (measured by a Pt-100 sensor placed one meter deep in the center of the pool) were measured for three days with 10-minute intervals [13]. The experimental database was used to test the following three different energy balance models (all, as previously described, implemented in TRNSYS):

- Model-A, which is the one proposed in this study, where the approach introduced by Shah [64] has been adopted to determine either forced or natural evaporation conditions.
- Model-B, which is the model from the previous point, where the only difference lies in the utilization of Eq. (16) to model the contributions of forced and natural evaporation, following the approach proposed by Lovell *et al.* [19].
- Benchmark model, which is the one already described earlier in this paper [16].

The three numerical models were employed to conduct dynamic simulations aimed at reproducing the observed water temperature fluctuations in the Spanish pool during the 72-hour monitoring period. As it is not known in which month of the year this monitoring period took place [13], distinct simulations were carried out for each of the three aforementioned tested models, assuming α_w values of 0.85, 0.855, and 0.86, respectively.

All additional assumptions that were taken into account for the validation analyses are described along with the definitions of the errors (MAE and MAPE) that are used to make the accuracy assessment of the new approach are detailed in SI 8.

At the end of this subsection, it is important to highlight that the wind speed values v_{wi} of the experimental dataset of Ruiz and Martínez [13] were directly used as inputs in the three models without applying any further corrections. These values, in fact, were locally measured by using an anemometer placed 50 cm above the water surface of the monitored pool. This measurement height, as already established, is considered appropriate for determining the wind speed values to be used in Richter's correlation [31]. Similarly, in this work, it is assumed that the wind speed values measured at this height could also be directly used in the Inan and Atayilmaz correlation [55] (i. e., Eq. (6) of the novel model). The validity of this assumption has been confirmed by the results of the analysis presented below, as the latest correlation was utilized for the first time with this study to simulate forced evaporation from an outdoor swimming pool.

2.5.2. Numerical analyses performed for the case study

As a case study to test the applicability of the new model for analysing the energy consumption of open-air swimming pools, reference was made to the data presented by Mousia and Dimoudi [5]. These authors conducted a study on 68 outdoor pools located in different sites in Greece (Climate Zones A, B and C), focusing on energy audits conducted at swimming pools located in athletic and sports centres, primarily under the ownership of the public sector, municipalities, or clubs. These facilities experience high visitor footfall irrespective of weather conditions, necessitating the installation of heating systems. The majority of the outdoor pools examined are of Olympic dimensions (measuring 50 m by 21 m, with a typical area of 1050 m^2) and operate with water temperatures ranging between 25 and 28 °C [5]. These pools are open for more than 9 months per year, typically from 8:00 or 9:00 a. m. until 10:00 or 11:00p.m. Only a small proportion (24 %) have night covers for water evaporation mitigation [5]. Of all the pools analysed, around 60 per cent (38 pools) are located in the most densely populated area of Greece, near Athens (Climate Zone B). In this particular zone of Greece, the total surface area of all the pools is 32,891 m^2 and is frequented by approximately 24,160 athletes per year [5].

In addition, out of the entire sample analysed (across all three climate zones), only 27 swimming pools remain open throughout all 12 months (of which only 8 use cover). [5]. In this respect, these pools are open either 300 or 350 days a year, depending on whether they are closed or open on Sundays (it should be noted that in Greece there are 14 public holidays per year during which the pools are definitely closed). The annual values of specific thermal energy consumption (SEC_{th}), obtained by analyzing the three-year consumption of the 27 pools, are presented in Fig. 5 as a function of operating pool water temperature values (between 25 and 28 °C), distinguishing them for the three climatic zones of Greece (diamonds for Zone A, squares for Zone B and circles for Zone C) [5]. This data shows variations in the SEC_{th} ranging from 1,306 to 3,940 kWh/m^2, with an average for the whole sample ofSEC_{th} = 2,247 kWh/m^2 [5]. Furthermore, of the 27 pools, 19 (pools where a cover is not used) have an average consumption ofSEC_{th} = 2,456 kWh/m^2, while 8 (where a cover is used) are characterized by aSEC_{th} = 1,827 kWh/m^2 [5]. From the analysis of this data, Mousia and Dimoudi [5] derived two key findings applicable to Greek outdoor Olympic swimming pools: 1) a 1.0 °C reduction in pool water temperature leads to an approximately 500 kWh/m^2 reduction in thermal energy consumption per year; 2) the use of an anti-evaporation cover results in an annual consumption reduction of approximately 25.60 %.

Mousia and Dimoudi [5] do not specify which of the 27 pools whose consumption data are shown in Fig. 5 are installations where a cover is used at night. However, they point out that the higher values of thermal energy consumption are related both to the lower ambient temperatures (in the case of Climate Zone C) and to the non-use of the anti-evaporation cover [5].

For example, in the case of swimming pools in Climate Zone B, which represent the most statistically significant sample, the consumption data show a relatively high dispersion, which can be attributed either to a lack of energy management of the structure or to the non-use of a cover [5].

In this work, hourly numerical simulations with the new TRNSYS model were used to simulate the annual heat consumption of outdoor Olympic swimming pools (both with and without the use of covers) located in Climate Zone B in Greece that operate for both 300 and 350 days/year. For this purpose, the data in Fig. 5 were used both for an initial calibration phase and as a benchmark to evaluate the capability of the new model, as explained below.

2.5.2.1. Preliminary analysis of the data. Firstly, as shown in Fig. 5, the data from Zone B was divided by identifying pools where the cover was most likely not used (green boxes in the figure) and those where it was used (yellow boxes in the figure). The procedure used for this identification is described in detail in SI 9. The consumption data marked B in the figure (blue square) was excluded from the analysis because it was considered unrepresentative. After this partitioning, the following linear regression (represented in the figure by a green dashed line) can be identified for open-air swimming pools where the cover is not employed:

$$SEC_{th} = 283.44 \cdot T_w - 5157.9 \quad (24)$$

which can be used to predict the energy consumption data with anMAE = 289.89 kWh/m^2 and a$MAPE$ = 12.21 %.

2.5.2.2. Model parameters and monthly variable inputs. In order to make the description more concise, all the assumptions made for the definition of the: 1) average hourly pool occupancy profile; 2) constant model parameters; 3) monthly model inputs (heating system switch-on, use of

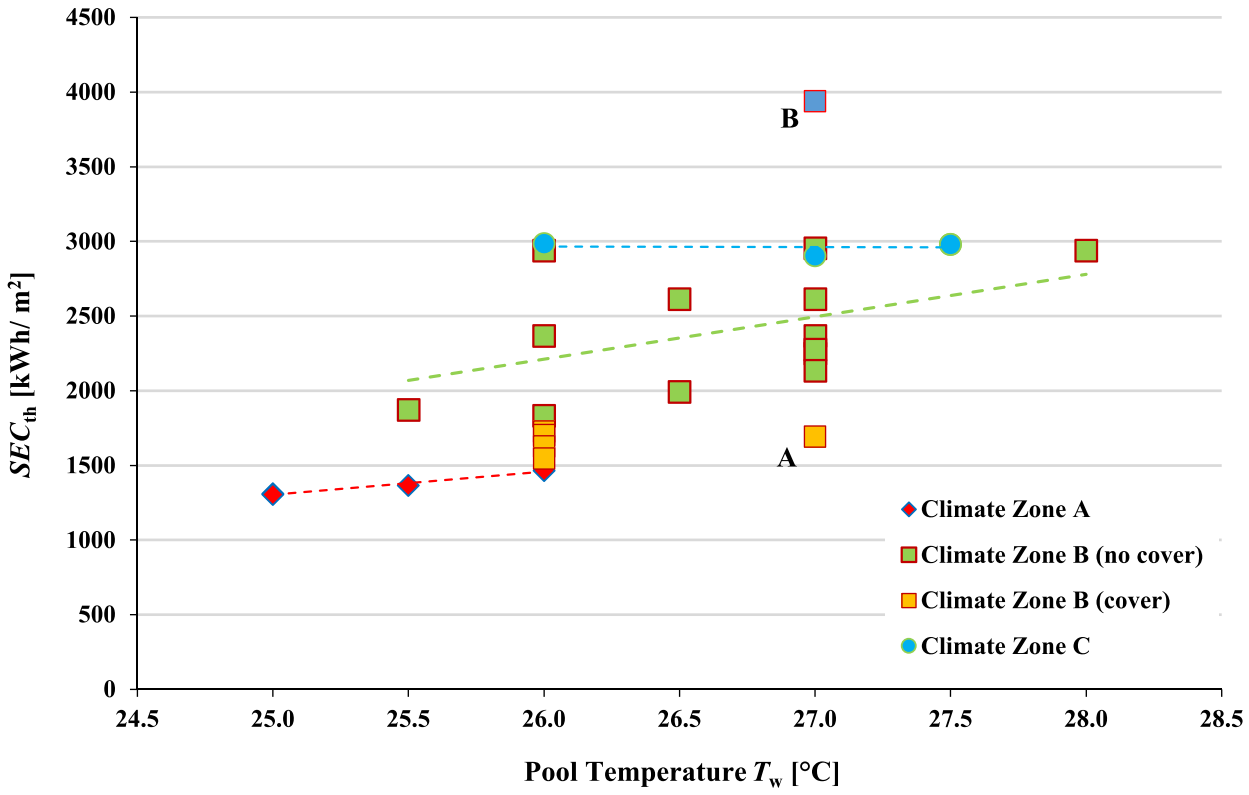

Fig. 5. Annual specific thermal energy consumptions for Greek outdoor swimming pool [5].

night cover and monthly pool renewal water temperature values T_{re}) are described in detail in SI 10.

2.5.2.3. Influence of climate data on model inputs. Before calibrating the model, setting plausible values for the parameters *ro* and *d* and using the TMY climate data of the Athens area, it was also possible to assess:

- the hourly variations of the solar absorption values α_w calculated for the outdoor pools (under the previous assumptions of $H_p = 2$ m and $\alpha_{fl} = 0.5$ and using the hourly values of G_h, G_b and θ_z from the TMY of Athens);
- the monthly values of the atmospheric stability class for the Athens area and the corresponding monthly average values of β_{rul} and β_{ur}.

2.5.2.4. Model calibration procedure. After previous preliminary analyses, the two model parameters, *ro* and *d*, which characterise the wind speed profile, were assumed to be free model parameters whose values were determined by the following model calibration procedure:

1. Firstly, for the data in Fig. 5, which refer to swimming pools in Climate Zone B operating at $T_w = 27$ °C and where the night cover is not used, an average value of $SEC_{th} = 2432.91$ kWh/m^2 per year was calculated.
2. Then, 11 hourly transient simulations were carried out varying *ro* between 0 and 1 (with intervals of 0.1) and for each of these 11 values of *ro*, the value of *d* that minimises the difference between the simulated and the above-calculated value of SEC_{th} was found. These simulations were carried out using the TRNSYS model considering swimming pools that have an operating water temperature of $T_w = 27$ °C, which are open 300 days/year and in which the cover is not used during the night.

2.5.2.5. Predictive simulations. After the calibration phase, annual hourly simulations with T_w varying between 26 and 28 °C (with a range of 0.5 °C) were carried out with the TRNSYS model for each of the 11 previously defined value pairs, for a total of 308 simulations, analysing the following cases:

- swimming pools that are open 300 days/year and where the cover is not used;
- swimming pools that are open 350 days/year and where the cover is not used;
- swimming pools that are open 300 days/year and where the cover is used;
- swimming pools that are open 350 days/year and where the cover is used.

To these simulations were added a further 77 simulations in which the unrealistic case of a pool with no users present was analysed for each of the 11 pairs of *ro* and *d* defined by the calibration procedure and by varying the T_w between 26 and 28 °C. These calculations were performed assuming pools open 300 days/year with no use of night cover.

The results of this first set of simulations were compared with the data in Fig. 5, obtained from the energy audits by Mousia and Dimoudi [5], in order to assess the predictive power of the model and to study, for example, the increase in annual consumption with increasing water temperature, the effect of the use of the cover in reducing the same consumption, the error committed when the presence of swimmers is neglected in the models, etc. In addition, in the case of a pool with a water temperature of $T_w = 26.5$ °C (equal to the average for Zone B) operating for 300 days/year, both the monthly distribution of heat demand and the percentage distribution of losses in the heating months were calculated, comparing pools using the cover with pools that do not use it.

2.5.2.6. Sensitivity analyses. In addition, the following parametric analyses were performed for the case of the swimming pool operating 300 days/year with the cover not in use:

- A total of 49 parametric simulations were carried out with *ro* fixed at 0.7 and both *d* and T_w varied in the range 0–0.474 m and 25–28 °C, respectively. The roughness parameter was set to a value$ro = 0.7$, which can be taken as representative of the area in which the pools around Athens are located, while$d = 0.474$ m is the value found by the best fit at$ro = 0.7$ in the calibration procedure described above.
- Similarly, the value of *d* was fixed at the best-fitting value (d=0.474 m) and a further 49 simulations were conducted by varying *ro* between 0 and 1 and T_w between 25 and 28 °C.
- Finally, a simulation was performed with$ro = 0$ and$d = 0$ (swimming pool located in a rural area with no obstacles around it) in order to simulate the most severe conditions in terms of the effect of wind on energy consumption.

The results of these analyses, for outdoor pools located in Climate Zone B, made it possible to define how the effect of local wind conditions (both the roughness of the area and the presence of obstacles around the pool) can influence the variations in annual consumption compared to the average for the zone for this type of facility.

3. Results and discussion

In the next two sub-sections, the results of the numerical analyses aimed at testing the new model presented with this work are shown and discussed, as well as those that were performed to analyse the case study, namely the energy analysis of outdoor Olympic swimming pools in Greece.

3.1. Results of the model validation

A comparison between the *MAE* and the *MAPE* values calculated from the results of the numerical simulations carried out with the three models (the new model in both versions A and B and the benchmark model) and the experimental measurements of the Spanish pool are summarised in the tables of SI 11. These results show in general that all three models are very accurate as they always present MAE and MAPE values below 0.12 °C and 0.52 %, respectively. All models are characterised by errors that decrease linearly as α_w increases in the range considered, indicating a certain sensitivity of the solution to this physical parameter. The best results were obtained at$\alpha_w = 0.86$ by Model A (MAE=0.056 °C and$MAPE = 0.23$ %), followed by the benchmark model (MAE=0.057 °C and$MAPE = 0.24$ %), and then Model B (MAE=0.093 °C and$MAPE = 0.39$ %).

The pool water temperature variations over time simulated by the three models in the case of$\alpha_w = 0.86$ have been plotted in Fig. 6 comparing them with the experimental data. When interpreting these results, it is important to note that the value of α_w is not constant and varies throughout the day depending on the altitude of the sun, being higher in the middle hours of the day.

Thus, the value of the solar absorptance at which the best results were obtained in this work is to be considered as a daily average value of the solar absorbance characterising that particular pool on those particular days of the year.

An interesting result obtained from this validation phase is that Model A is more accurate than Model B in simulating pool temperature variations. This observation gives an indication that the approach proposed by Shah [64] to model the contributions of natural and forced evaporation seems to work better than that proposed by Lovell *et al.* [19] using Eq. (9).

On the other hand, the deviation between the errors obtained with Model A and the benchmark model, as shown by the results obtained, is rather small. However, in the opinion of the authors, the second model is generally too simplistic because, on the one hand, it does not take into account the possibility of water evaporation by free convection (a situation that occurred several times during the monitoring of the Spanish swimming pool) and, on the other hand, it does not take into account the effect of relative humidity in the correlation used to estimate T_{sky}. The differences between Model A and the benchmark model are most evident when looking at the results shown in the pie chart in Fig. 7. This shows the percentage distribution of thermal losses between the two models. These values refer only to the hours in which the water temperature of the pool T_w was higher than the air temperature T_a (a situation closer to that of a heated outdoor pool in winter). The analysis of the numerical results made it possible to assess that, compared to Model A, the benchmark model underestimates evaporative and convective losses by 8 % and 14 %, respectively, while overestimating radiation losses by around 23.41 %. These differences, especially those related to evaporation, can lead to inaccurate assessments when, for example,

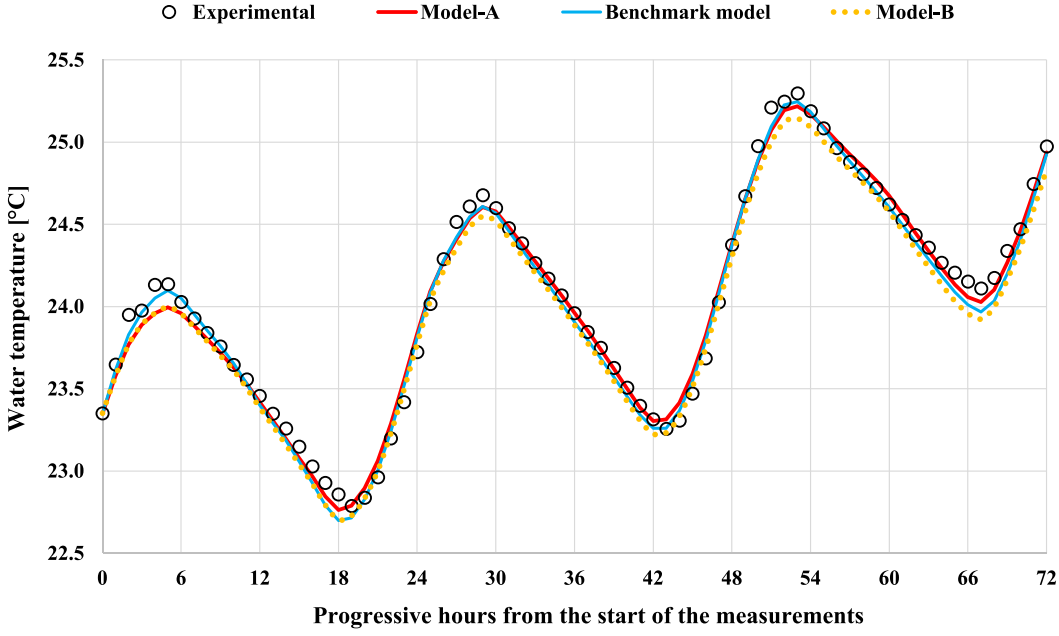

Fig. 6. Comparison of measured Spanish swimming pool water temperature data [13] with those simulated using the three numerical models (Model A, Model B and Benchmark).

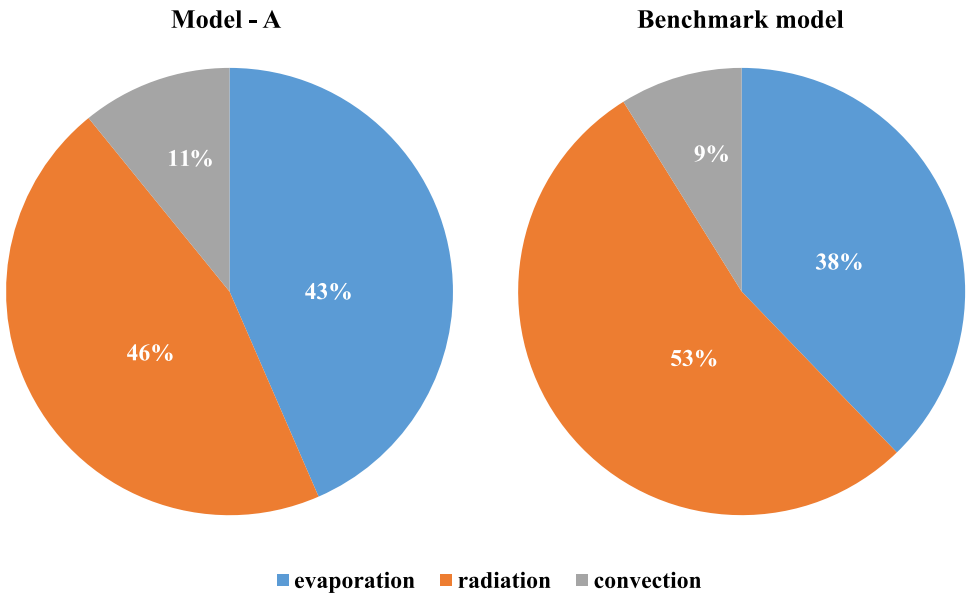

Fig. 7. Percentage distribution of the different pool heat losses calculated (for$T_w > T_a$) with Model A and the benchmark model respectively.

annual simulations are attempted to estimate both the effect of night cover and the effect of the presence of swimmers in reducing or increasing the total evaporative heat losses of an outdoor pool.

The main result of the numerical analyses aimed at validating the new model proposed with this work shows that through its use, it was possible to predict with great accuracy the temperature variations measured by Mousia and Dimoudi [5] for the Spanish pool, with lower errors even than the reference model that has been the best performing for this dataset until now. This result also gives an indirect indication that the choice of$z = 0.5$ m as the reference height for wind speed measurement for the Inan and Atayilmaz correlation [55], is indeed appropriate. Future experimental studies on the evaporation rate by forced convection from swimming pools may further validate this preliminary assumption.

Using the same parameterization, it was also possible to estimate that the average daily evaporation rate in the Spanish swimming pool is $3.63{\cdot}10^{-3} = m^3/(m^2{\cdot}day)$. In other words, the water level in the pool decreased by approximately 1.1 cm over the span of three days.

3.2. Results of the numerical analyses of the case study

A first result of the application of the numerical model to the case of the Greek outdoor Olympic swimming pools, considering as input climate variables based on the TMY data for Climate Zone B, was the calculation of the hourly variations of solar absorptance of these facilities for one year.

These results, that have been summarised in the table in SI 12, show that this physical parameter is not constant over time, but rather, once the water level in the pool H_p and the value of the floor and walls α_{fl} are fixed, it must be calculated using appropriate models that take into account solar heights and, diffuse and direct components of solar radiation, which naturally vary from hour to hour during the year. In this respect, there is no real justification for assuming a solar absorbance value of precisely$\alpha_w = 0.85$ as is frequently found in many models presented in the literature [8,13,14,16].In addition to the analysis of the temporal variations of the solar absorption from the same simulations, it was possible to calculate the hourly variations of the atmospheric stability class, estimated using the Pasquill criterion for Climate Zone B. These results have been summarised in the graph depicted in SI 13. The hourly values of the stability classes obtained also made it possible to calculate the hourly variations of the two coefficients β_{ru} and β_{ur} necessary to define the exponent β of the wind speed profile model adopted in this study (Eq. (22).

Finally, the results of the 11 parametric simulations for the calibration of the model are also presented in detail in SI 14 in terms of *d* as a function of *ro*.

3.2.0.1. Results of predictive simulations

The curves of SEC_{th} as a function of T_w obtained through simulations for each of the defined scenarios are depicted in Fig. 8, along with data from the energy audits carried out by Mousia and Dimoudi [5]. The curves in Fig. 8 show the main result of this work, namely the ability of the proposed new model to predict the annual consumption of the analysed pools over the whole range of T_w temperatures analysed. In particular, the continuous green curve (relating to pools operating 300 days/year where the enclosure is not used), obtained from simulations with the pool model calibrated on data of$T_w = 27$ °C, allows the fit of pool consumption data over the entire range of water temperatures studied with an$MAE = 289.085$ kWh/m^2 and a$MAPE = 11.91$ % (calculated using data from both numerical simulations and energy audits).

These error values are slightly lower than those obtained using the linear correlation described by Eq. (24), whose constants were defined by fitting all the energy audit data (corresponding to T_w values between 25.5 and 28 °C) and not only those corresponding to$T_w = 27$ °C, as in the case of the curve obtained by the simulation model. The function predicting the annual SEC_{th} of the pools as a function of T_w, which can be calculated from this first set of numerical results, can be approximated by the following quadratic relation:

$$SEC_{th} = 12.645{\cdot}T_w^2 - 422.74{\cdot}T_w + 4629.1 \quad (25)$$

This correlation can be used, as a first approximation, to define the annual thermal energy consumption of outdoor Olympic swimming pools in which no night cover is used in climatic zones similar to Athens. Using this curve, it is also possible to deduce an important fact for these facilities, that is, for every 1 °C increase in operating water temperature, an increase in annual consumption of approximately 124 kWh/m^2 can be expected (corresponding to about 11 %).

The continuous yellow curve in Fig. 8 was obtained with the model calibrated with the same data as before (energy consumptions of pools without the cover operating at T_w), but by carrying out simulations with the model considering 300 days/year of opening and the use of the cover during the closing hours of the pool. As can be seen, this curve, which is

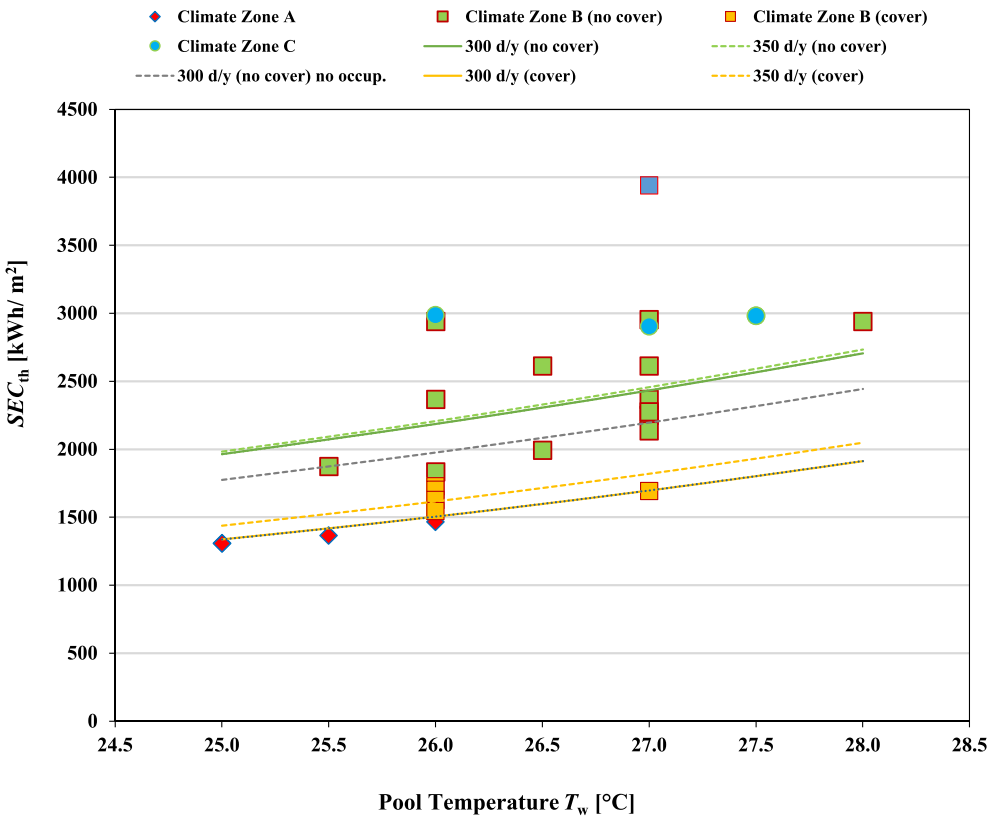

Fig. 8. Comparison of the results of numerical simulations (for climate Zone B of Greece) and data from energy audits of Olympic outdoor swimming pools.

significantly lower than the previous one (the continuous green one), was able to predict with a good approximation (*MAE*=183.35 kWh/m^2 and*MAPE* = 10.86 %) the energy audit data referring to pools using the cover operating with water temperatures between 26 and 27 °C. Also in this case, it is possible to propose a correlation useful to estimate, as a first approximation, the annual thermal energy consumption of outdoor pools where the night cover is regularly used:

$$SEC_{th} = 12.088 \cdot T_w^2 - 448.32 \cdot T_w + 4989.4 \quad (26)$$

An important result obtained by comparing the two curves (described by Eq. (25) and Eq. (26), respectively) is that the use of the anti-evaporation cover allows an average annual energy saving of about 30.57 % compared to not using it. The latter value is higher than the savings rate of 25.60 % obtained by Mousia and Dimoudi [5] when analysing the same energy audit data without the support of a numerical analysis model.

Simulation results in the case of pools that use and do not use cover but are open for 350 days/year are represented in Fig. 8 by the two SEC_{th}-T_w curves with green and yellow dashed lines, respectively. The first curve, as can be seen from the same figure, is almost superimposable on that of pools where the cover is not used and are open for 300 days/year. The second curve, the one for the case of pools where the cover is used and are open for 350 days/year, is higher than that for pools open for 300 days/year. This difference is due to the fact that for pools that are closed on Sundays, the use of the cover allows a reduction in consumption compared to the case where these pools are open on Sundays and the cover is used only during the night hours. The dashed yellow curve of Fig. 8 (obtained from the simulations for pools using the cover and open 350 days/year) fits the corresponding thermal energy consumption data with error values of*MAE* = 81.15 kWh/m^2 and an*MAPE* = 4.84 %. These error values are lower than those obtained in the previous analyses. It can be concluded that most of this consumption data refer to facilities that are also open on Sundays. For example, for the case study presented by Mousia and Dimoudi [5] related to a swimming pool operating atT_w = 26 °C for 350 days/year for which the cover is used at night, the numerical model predicts aSEC_{th} = 1,616.30 kWh/m^2 which is quite close (*MAE*=71.70 kWh/m^2 and a*MAPE* = 4.84 %) to the value of defined by the energy audit of this facility (SEC_{th}=1,688 kWh/m^2).

Finally, the dashed grey curve in Fig. 8 has been plotted from the numerical results of the swimming pool model (calibrated with the previous parameters) assuming the unrealistic case of no swimmers. This curve (which refers to facilities operating with water temperatures between 25 °C and 28 °C, with no use of covers) is located below the continuous green curve and shows another important result of this work, which is that neglecting the presence of swimmers in the energy consumption prediction models (as most studies of outdoor pools in the literature do) leads to an error in the prediction of annual consumption, which can be estimated at around 10 % in the case of the data used here. This result justifies the effort made in this paper to define a model that attempts to predict the increase in water evaporation rate as a function of the number of athletes in the case of outdoor pools.

In order to analyse the results obtained from numerical simulations for outdoor Olympic swimming pools in the Athens area in more detail, the case of pools operating atT_w = 26.5 °C and open 300 days/year is discussed below. Fig. 9 shows, for example, the hourly variation of the heating energy demand $\dot{Q}_{heat}$ for a swimming pool where the cover is not used.

In the same figure, this dataset is juxtaposed with the hourly variations of the following parameters: the pool water temperature T_w, the air temperature T_a, and apparent sky temperature T_{sky} (which, in this region of Greece, exhibit annual mean values ofT_a = 16.54 °C andT_{sky} = 7.94 °C, respectively). According to the simulation results, the annual thermal energy demand for pools operating as described would amount to 2.42 GWh (equivalent to aSEC_{th} = 2306 kWh/m^2). The peak thermal energy demand would reach$\dot{Q}_{heat}$ = 1,215 kW, with an annual average of

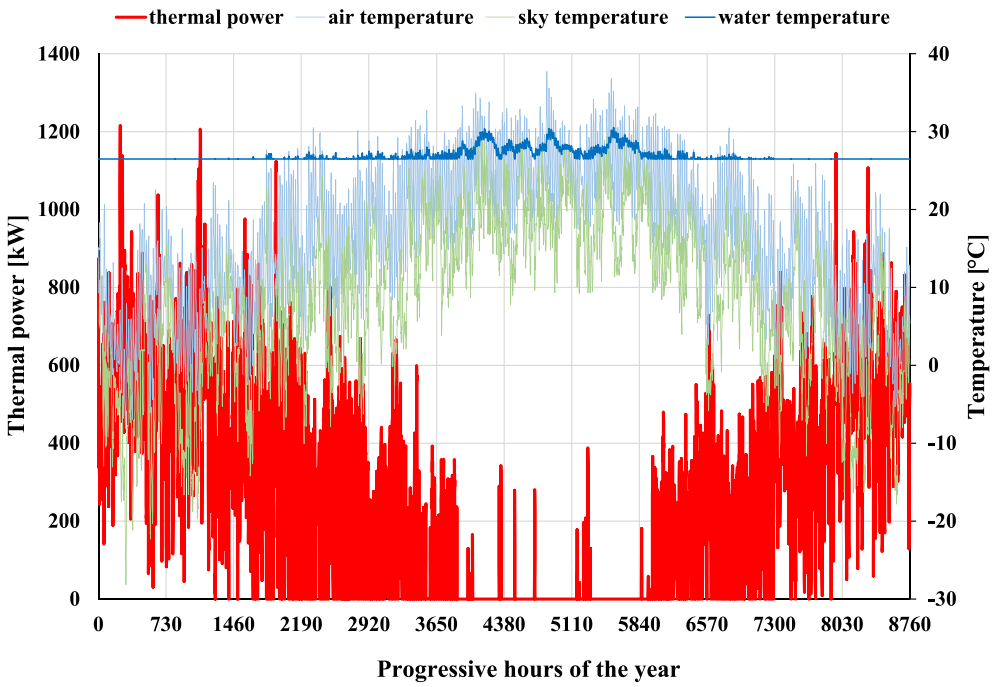

Fig. 9. Hourly variations of: $\dot{Q}_h$ (for pools withT_w = 26.5 °C, open 300 days/year and no cover), T_w, T_a and T_{sky} (for Climatic Zone B of Greece).

approximately$\dot{Q}_{heat}$ = 446 kW. Furthermore, the yearly volume of water evaporated is estimated to be around 3,194 m^3, corresponding to an average hourly evaporation rate of$\dot{E}_p = 8.33{\cdot}10^{-3}$ $m^3/(m^2{\cdot}day)$.

As can be seen in Fig. 9, during the summer period (between June and September), the heating demand decreases to almost zero, as the thermal input contributions due to both solar radiation and rising air temperature allow the water temperature to be maintained at an average ofT_w = 27.86 °C (which is higher than the set temperatureT_w = 26.5 °C).

The simulation result also shows that during the summer season, the water temperature can exceed the comfort temperature ofT_w = 28 °C in the middle hours of the day. For this reason, for open-air swimming pools located in climatic zones similar to that of Athens, it is common practice to increase the rate of replacement water from the aqueduct in order to cool the pool water.

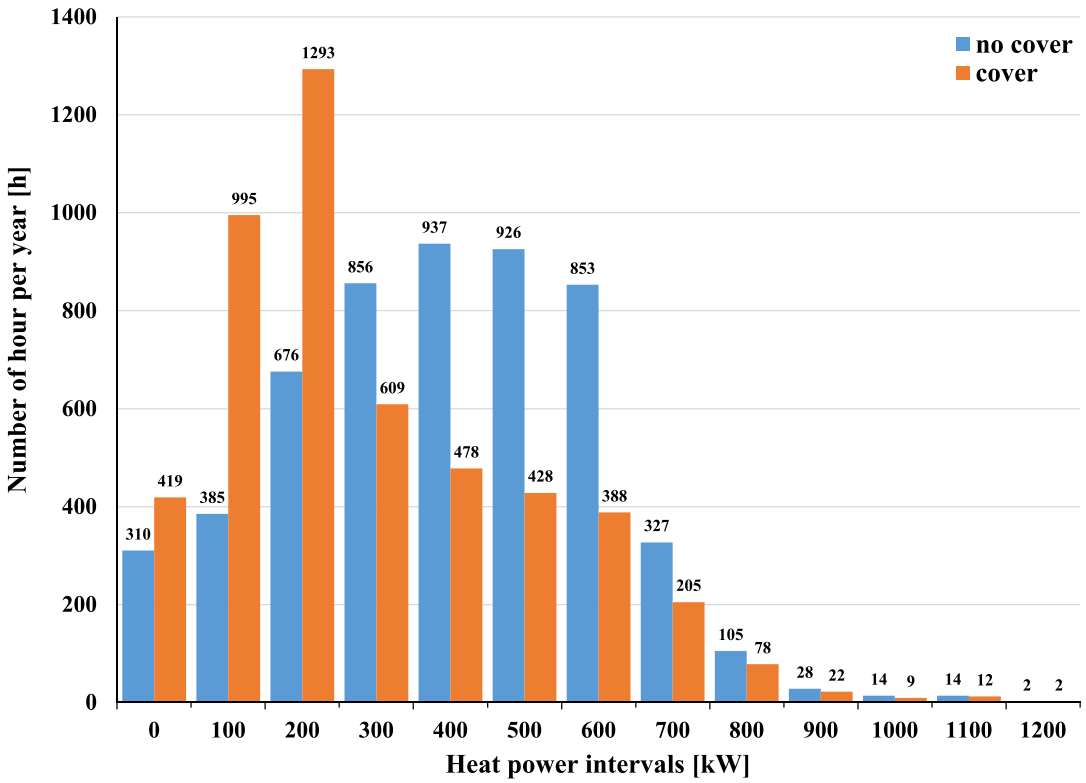

Fig. 10. Frequency distributions of thermal power demand $\dot{Q}_{heat}$ in the two cases of use and non-use of the cover (pools withT_w = 26.5 °C, open 300 days/year).

If, on the other hand, the use of a night cover is considered for the same type of swimming pool, the simulations give: an annual heat demand of 1.67 GWh (corresponding to SEC_{th} = 1,598 kWh/m^2), a peak heat demand of $\dot{Q}_{heat}$ = 1,215 kW (identical to the case of the pool without cover) and an average annual heat output of $\dot{Q}_{heat}$ = 192 kW. In this case, the volume of water evaporated in a year would be about 2303 m^3, which corresponds to an average hourly evaporation rate of about $\dot{E}_p$ = 6.01·10^{-3} m^3/(m^2·day). Comparison of the numerical results described above shows that the use of night covers in outdoor swimming pools achieves a reduction in evaporated water volume of around 28 %, which corresponds to a reduction in the annual heat demand of around 31 %.

For a more detailed comparison between the two cases, Fig. 10 shows histograms representing the frequency distributions of the thermal demand in the two cases of use and non-use of the cover. These diagrams show the thermal power intervals in the abscissa and the number of hours in which they occur each year in the ordinate. As pointed out by Lovell *et al* [19], this type of diagram is fundamental from the point of view of the possibility of carrying out energy and efficiency analyses for this type of facility. Both histograms show that the peak thermal power demand $\dot{Q}_{heat}$ (between 1200 and 1330 kW) occurs for only 2 h per year in both cases. On the other hand, in the case of a pool that is not equipped with a cover, the most frequent thermal power demand $\dot{Q}_{heat}$ is between 400 and 500 kW (937 h/year). This result, as well as the overall frequency profile in Fig. 10, is very similar to that obtained by Lovell *et al* [19] using their numerical model for the outdoor Olympic pool in Perth, Australia [19]. On the other hand, the regular use of the night cover not only reduces the total thermal demand of the pools, but also significantly changes the frequency profiles of the thermal powers $\dot{Q}_{heat}$. This can be seen from the data in Fig. 10, where the most frequent $\dot{Q}_{heat}$ (1293 h/year) shifts to lower levels, between 200 and 300 kW, compared to the previous case.

This type of information, which can be obtained from numerical models similar to the one presented in this study, is fundamental for the design and optimisation of efficient systems for this type of sports and recreational facility. The comparison between the two cases is also illustrated in Fig. 11, which shows the monthly values of the SEC_{th}. From these histograms it is possible to note what has already been described above, namely that the greatest thermal demands occur in the winter period (in the months of December and January) and are almost zero in the two summer months of July and August.

In particular, for swimming pools without a cover, the SEC_{th} in December is approximately SEC_{th} = 413 kWh/m^2, which is reduced to SEC_{th} = 303 kWh/m^2 if a cover is used. In the months between June and September, the monthly SEC_{th} are identical because the night cover is not used. Analysing the results of Fig. 11 in more detail, it can be estimated that the use of coverage leads to a percentage reduction in monthly SEC_{th} that increases in the first phase of the year, from 27 % in January to 58 % in May, and decreases after the summer months, from 40 % in October to 30 % in December.

Again, for the case of a pool operating at T_w = 26.5 °C for 300 days/year and where the cover is not used, Fig. 12 shows the daily values of the different components that constitute the thermal losses of the pool: evaporation, convection, radiation and those due to water refilling. From these graphs it can be seen that the losses increase significantly during the winter period and that the largest contribution is made by the losses due to evaporation of water from the pool. A more detailed analysis of the results shows that 70 % of this component is due to forced convection evaporation and 30 % to natural convection. This result confirms what has already been stated by the most recent work presented in the literature [19], namely that energy balance models for outdoor swimming pools cannot disregard the modelling of the evaporation component under natural convection conditions.

Fig. 13 illustrates the annual percentage distribution of thermal loss components for the non-use and use of the cover. This comparison only considers periods where the pool heating system was active throughout the year analysed. For uncovered swimming pools, the loss distribution observed is similar to that described in existing literature for outdoor Olympic pools [9,19]. Evaporation accounts for the highest proportion of losses (at least 50 %), while convection (19 %) and radiation (23 %) contribute a relatively equal proportion with a slight prevalence of the latter component.

The percentage of the final component, which pertains to the pool's make-up water sourced from the aqueduct, may vary depending on the

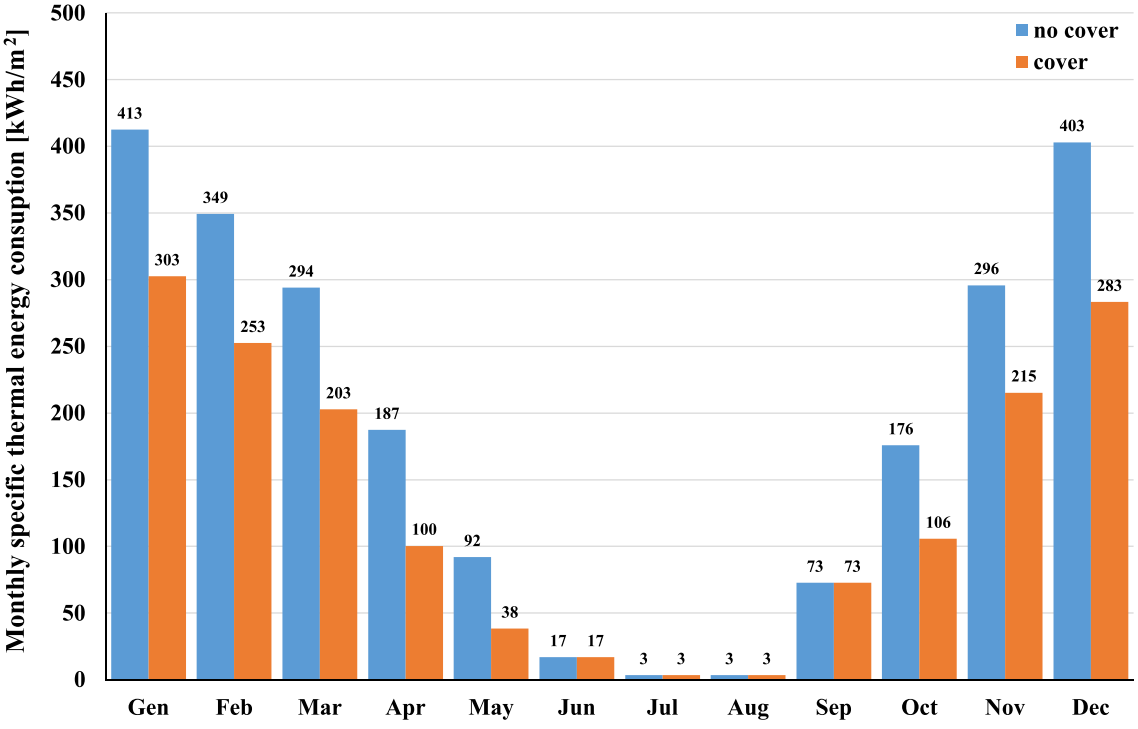

Fig. 11. Monthly SEC_{th} values in the case of pools where the cover is and is not used (pools with T_w = 26.5 °C, open 300 days/year).

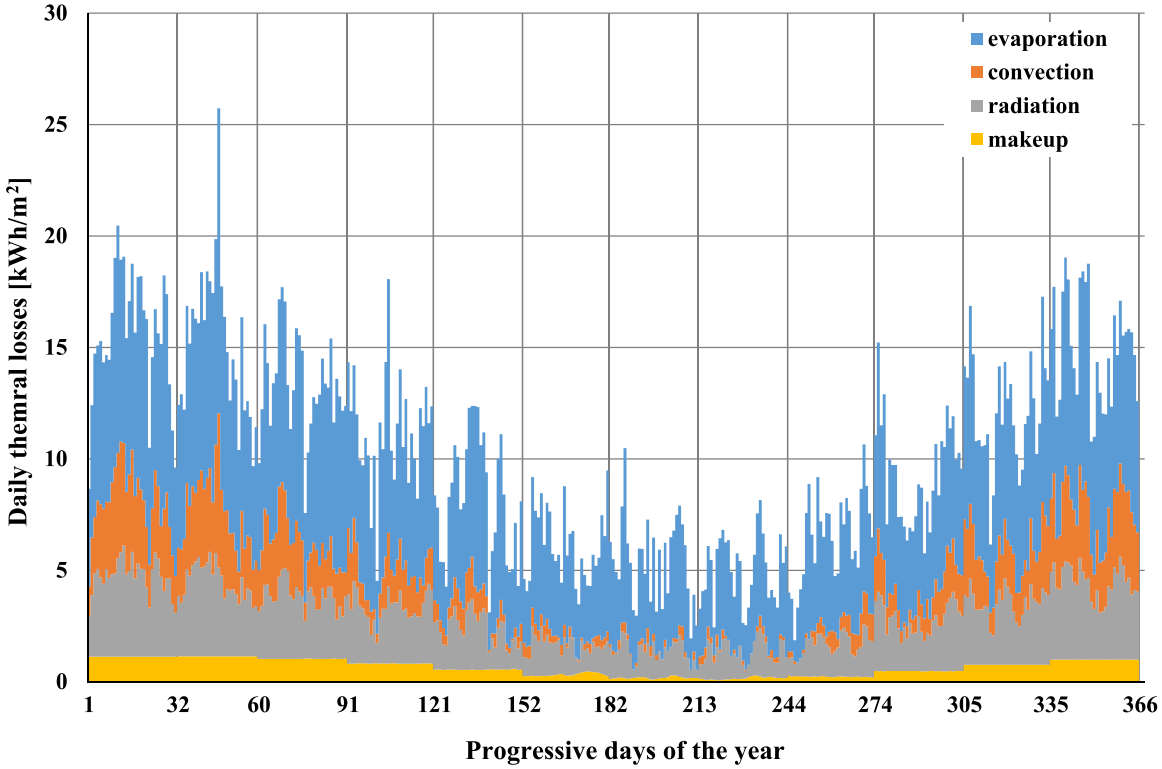

Fig. 12. Daily values of the different components of heat loss from a pool operating at a water temperatureT_w = 26.5 °C for 300 days/year with no cover use.

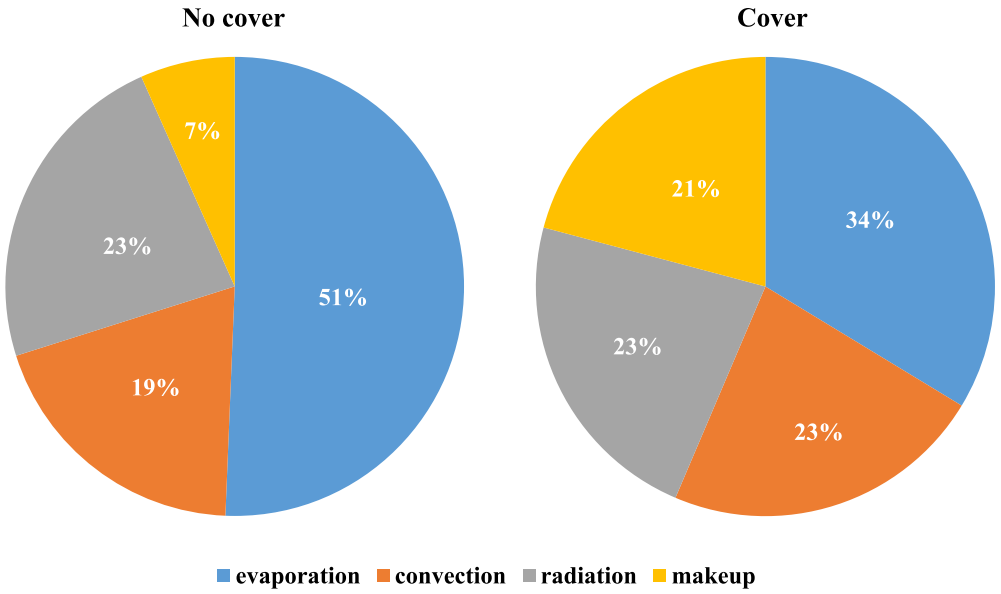

Fig. 13. Percentage distribution of the different pool heat losses calculated over the heating period in the two cases of pools where the night cover is not used and is used.

water renewal percentage F_{re} and the temperature discrepancy between the pool water T_w and the aqueduct water T_{re}. Using the cover at night, as illustrated in Fig. 13, reduces evaporation losses by equalising the distribution of thermal losses among all components. However, compared to other factors, evaporation losses are still significant.

3.2.0.2. Results of sensitivity analyses

Finally, this article discusses the sensitivity analyses carried out to examine the influence of parameters *ro* and *d* on the numerical solution of SEC_{th} curves as a function of water temperature T_w. All results shown below refer to the case of swimming pools operating 300 days/year on which the night cover is not used. The first set of simulations, as explained earlier, involved setting the model parameter *d* value at 0.474 m, which describes the average height of obstacles found around the pool site. Then, the value of the roughness parameter *ro* was varied in the range 0–1. The simulation results were plotted alongside the energy audit data for the Greek pools in Fig. 14, marked with black dashed lines. The findings indicate that as the value of *ro* decreases, thermal

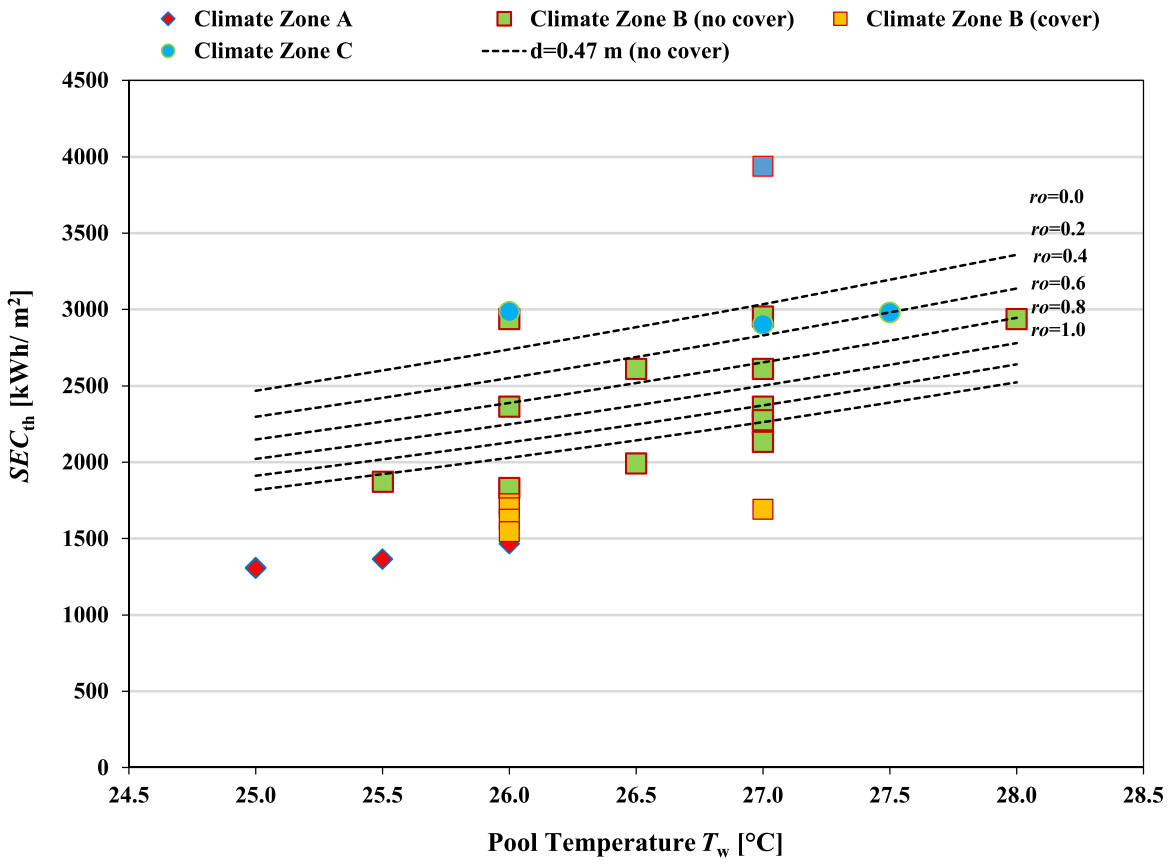

Fig. 14. Curves of SEC_{th} as a function of water temperature T_w for fixed$d$ = 0.474 and *ro* varying between 0 and 1 m (dashed lines) along with audit data for swimming pools in Greece.

consumption around the pool increases, with a fixed *d*-value representing the type of structure surrounding the pool. Therefore, in areas with less roughness, where wind speeds rise, thermal losses increase as one moves further away from an urbanised area (*ro*=1). What makes these results noteworthy is that the curves plotted encompass most of the audit data (see Fig. 14). Thus, this latter observation suggests that the variation in annual swimming pool energy consumption recorded during the survey campaign may simply be related to the different local roughness conditions of the areas where the different structures are built.

Another set of simulations was conducted by configuring the parameter *ro* to have a value of 0.7. This value, as already mentioned, was assumed by trying to identify the average roughness of the areas where the pools are located around Athens. Then the value of the average obstacle height parameter *d* was varied in the range of 0 and *d* = 0.474 m. The curves SEC_{th} as a function of T_w obtained as the simulation results, are displayed in Fig. 15 with dashed black lines, accompanied by the energy audit data of the Greek swimming pools. It can be inferred from these findings that with the same average roughness of the area in which the pools are built, as the height of the obstacles *d* around them decreases, the effects of wind on heat loss increase.

Finally, the last round of simulations was conducted using two parameters of*ro* = 0 and*d* = 0.474 m, signifying an outdoor swimming pool situated away from the city centre (*ro*=0) and free from any obstructions. The red dashed curve illustrated in Fig. 15 precisely exhibits the results of these simulations and represents the upper limit curve for the annual energy consumption that can be estimated for the analysed swimming pool case.

Fig. 15 reveals a surprising discovery: the energy consumption figure that was marked with letter B in Fig. 5, excluded from previous analyses, falls exactly on this curve. This finding suggests that high energy consumption in this specific pool may not be solely attributed to poor energy management or lack of use of the cover, but also to its possible location in an area particularly exposed to the effects of wind.

In summary, the data presented in Figs. 14-15 indicate that the impact of local wind conditions, which is primarily influenced by atmospheric stability, surface roughness, and obstructing objects, has a significant effect on the magnitude of thermal losses and subsequently, on energy consumption for outdoor structures of this type. Thus, an objective assessment of consumption remains unachievable, even by the most advanced numerical models, unless model parameters undergo careful calibration. For this calibration, either local wind measurements or consumption data from pre-existing pools within the study area must be available. In this paper, the latter approach was followed.

4. Conclusions

This paper presents a new energy balance model of outdoor swimming pools aimed at defining the thermal energy demand for their heating. This model incorporates the approach introduced by Wu *et al.* [61] for calculating the water solar absorption and the use of the Bowen's ratio for the calculation of the convective losses from the evaporation. At the same time, it introduces the following innovations for outdoor pool models: the use of the recent correlation of Inan and Atayilmaz [55] for the calculation of evaporation by forced convection, a new model of the evaporation enhancement factor as a function of pool occupancy, the use of the recent correlation proposed by Guo *et al.* [50] for the calculation of sky temperature, and an approach to wind speed correction that takes into account variations in atmospheric stability conditions, surface roughness and the presence of obstacles in the pool environment. Results of the numerical analyses presented in this paper showed that:

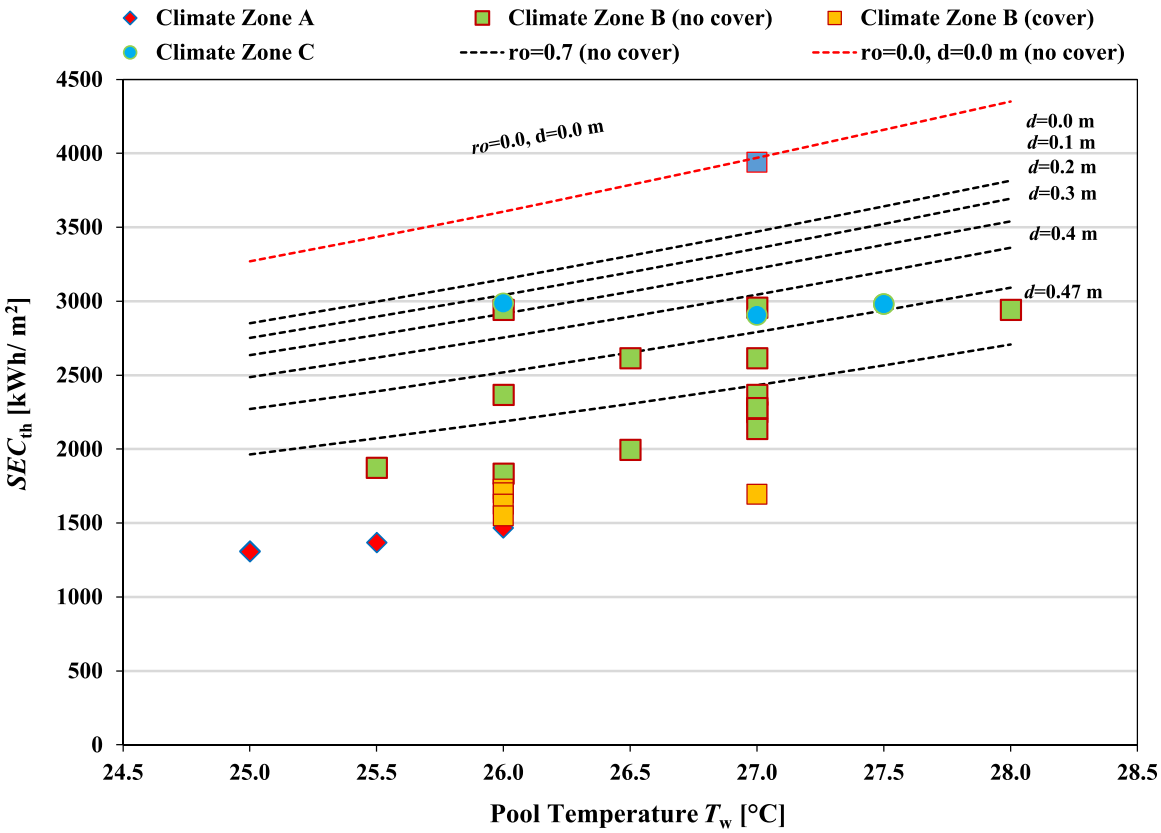

Fig. 15. Curves of SEC_{th} as a function of water temperature T_w for different combinations of d and ro (dashed lines) along with audit energy data for swimming pools in Greece.

- the proposed model allows the prediction of water temperature variations recorded for a Spanish swimming pool [13] with a lower error (MAPE = 0.23 %) than other models proposed in the literature for the same case study [16].
- The method proposed by Shah [64] for modelling the combination of forced and natural evaporation seems to be more accurate than the one proposed by Lovell *et al.* [19].
- The proposed model allows the prediction of the annual thermal energy demand assessed for outdoor Olympic swimming pools in Greece [5] (operating at water temperature ranging between 25 and 26 °C) with a MAPE of less then12%.
- For the average case of an Greek outdoor swimming pool operating at 26.5 °C for 300 days per year and in which the cover is not used, it is possible to estimate an annual specific thermal energy consumption of 2306 kWh/m^2. When the cover is used, the same consumption is reduced to 1.598 kWh/m^2.
- Neglecting the pool occupancy factor in energy balance models leads to an underestimation of annual energy demand by up to 10 %.
- On average, the largest heat loss in outdoor pools is due to evaporation (50 %), followed by radiation (23 %), then convection (19 %) and finally water refilling (7 %).
- At least 30 % of the evaporative losses take place through natural convection. This suggests that accurate results in energy balance modelling of outdoor pools can only be achieved by including this heat transfer mechanism.
- Reducing the operating water temperature by 1 °C leads to a reduction in energy consumption of around 11 %, and that the use of night covers leads to energy savings of up to around 30 %.

Finally, the results of a series of numerical sensitivity analyses showed that the effect of local wind conditions plays a fundamental role in the level of energy consumption for outdoor structures of this type. Therefore, even with the most advanced numerical models, an objective assessment of consumption is not possible unless the model parameters are carefully calibrated using local wind measurements or consumption data from existing pools in the study area.

CRediT authorship contribution statement

Alessandro Buscemi: Conceptualization, Investigation, Methodology, Software, Writing - Original Draft. **Alessandro Biondi:** Conceptualization, Investigation, Software, Writing - Review & Editing, Formal analysis. **Pietro Catrini:** Conceptualization, Investigation, Software, Writing - Review & Editing, Formal analysis. **Stefania Guarino:** Conceptualization, Investigation, Software, Writing – review & editing, Formal analysis. **Valerio Lo Brano:** Supervision, Investigation, Validation.

Declaration of competing interest

The authors declare the following financial interests/personal relationships which may be considered as potential competing interests: [Valerio Lo Brano reports financial support was provided by European Union. If there are other authors, they declare that they have no known competing financial interests or personal relationships that could have appeared to influence the work reported in this paper].

Data availability

Data will be made available on request.

Acknowledgments

This study was developed in the framework of the research activities

carried out within the Project “Network 4 Energy Sustainable Transition—NEST”, Spoke 1., Project code PE0000021, funded under the National Recovery and Resilience Plan (NRRP), Mission 4, Component 2, Investment 1.3— Call for tender No. 1561 of 11.10.2022 of Ministero dell`Universita` e della Ricerca (MUR); funded by the European Union—NextGenerationEU; the possibility of using a Dish-Stirling type solar concentrator to supply thermal power to an outdoor swimming pool in order to minimise conventional heat demand is being investigated.

Appendix A. Supplementary data

Supplementary data to this article can be found online at https://doi.org/10.1016/j.enconman.2024.118152.

References

[1] Trianti-Stourna E, Spyropoulou K, Theofylaktos C, Droutsa K, Balaras CA, Santamouris M, et al. Energy conservation strategies for sports centers: Part B. Swimming pools. Energy Build 1998;27. https://doi.org/10.1016/s0378-7788(97)00041-8.
[2] Kampel W, Aas B, Bruland A. Characteristics of energy-efficient swimming facilities - a case study. Energy 2014;75. https://doi.org/10.1016/j.energy.2014.08.007.
[3] Kampel W, Aas B, Bruland A. Energy-use in Norwegian swimming halls. Energy Build 2013;59. https://doi.org/10.1016/j.enbuild.2012.11.011.
[4] Saari A, Sekki T. Energy Consumption of a Public Swimming Bath. Open Constr Build Technol J 2008;2. https://doi.org/10.2174/1874836800802010202.
[5] Mousia A, Dimoudi A. Energy performance of open air swimming pools in Greece. Energy Build 2015;90:166–72. https://doi.org/10.1016/j.enbuild.2015.01.004.
[6] Li Y, Nord N, Huang G, Li X. Swimming pool heating technology: a state-of-the-art review. Build Simul 2021;14:421–40. https://doi.org/10.1007/s12273-020-0669-3.
[7] Delgado Marín JP, Garcia-Cascales JR. Dynamic simulation model and empirical validation for estimating thermal energy demand in indoor swimming pools. Energy Effic 2020;13. https://doi.org/10.1007/s12053-020-09863-7.
[8] Buonomano A, De Luca G, Figaj RD, Vanoli L. Dynamic simulation and thermo-economic analysis of a PhotoVoltaic/Thermal collector heating system for an indoor–outdoor swimming pool. Energy Convers Manag 2015;99:176–92. https://doi.org/10.1016/j.enconman.2015.04.022.
[9] Hahne E, Kübler R. Monitoring and simulation of the thermal performance of solar heated outdoor swimming pools. Sol Energy 1994;53. https://doi.org/10.1016/S0038-092X(94)90598-3.
[10] Al KD. Comparison of swimming pools alternative passive and active heating systems based on renewable energy sources in Southern Europe. Energy 2015;81:738–53.
[11] Lugo S, Morales LI, Best R, Gómez VH, García-Valladares O. Numerical simulation and experimental validation of an outdoor-swimming-pool solar heating system in warm climates. Sol Energy 2019;189. https://doi.org/10.1016/j.solener.2019.07.041.
[12] Molineaux B, Lachal B, Guisan O. Thermal analysis of five outdoor swimming pools heated by unglazed solar collectors. Sol Energy 1994;53. https://doi.org/10.1016/S0038-092X(94)90599-1.
[13] Ruiz E, Martínez PJ. Analysis of an open-air swimming pool solar heating system by using an experimentally validated TRNSYS model. Sol Energy 2010;84. https://doi.org/10.1016/j.solener.2009.10.015.
[14] Lam JC, Chan WW. Life cycle energy cost analysis of heat pump application for hotel swimming pools. Energy Convers Manag 2001;42. https://doi.org/10.1016/S0196-8904(00)00146-1.
[15] Szeicz G, McMonagle RC. The heat balance of urban swimming pools. Sol Energy 1983;30. https://doi.org/10.1016/0038-092X(83)90154-8.
[16] Zsembinszki G, Farid MM, Cabeza LF. Analysis of implementing phase change materials in open-air swimming pools. Sol Energy 2012;86. https://doi.org/10.1016/j.solener.2011.10.028.
[17] Sheng L, Su L, Zhang H, Li K, Fang Y, Ye W, et al. Numerical investigation on a lithium ion battery thermal management utilizing a serpentine-channel liquid cooling plate exchanger. Int J Heat Mass Transf 2019;141:658–68. https://doi.org/10.1016/j.ijheatmasstransfer.2019.07.033.
[18] Sheng L, Zhang H, Su L, Zhang Z, Zhang H, Li K, et al. Effect analysis on thermal profile management of a cylindrical lithium-ion battery utilizing a cellular liquid cooling jacket. Energy 2021;220:119725. https://doi.org/10.1016/j.energy.2020.119725.
[19] Lovell D, Rickerby T, Vandereydt B, Do L, Wang X, Srinivasan K, et al. Thermal performance prediction of outdoor swimming pools. Build Environ 2019;160. https://doi.org/10.1016/j.buildenv.2019.106167.
[20] Woolley J, Harrington C, Modera M. Swimming pools as heat sinks for air conditioners: model design and experimental validation for natural thermal behavior of the pool. Build Environ 2011;46. https://doi.org/10.1016/j.buildenv.2010.07.014.
[21] Poós T, Varju E. Mass transfer coefficient for water evaporation by theoretical and empirical correlations. Int J Heat Mass Transf 2020;153. https://doi.org/10.1016/j.ijheatmasstransfer.2020.119500.
[22] Shah MM. Methods for calculation of evaporation from swimming pools and other water surfaces. ASHRAE Conf., vol. 120, 2014.
[23] Sartori E. A critical review on equations employed for the calculation of the evaporation rate from free water surfaces. Sol Energy 2000;68. https://doi.org/10.1016/S0038-092X(99)00054-7.
[24] Dalton J. Experimental essays, on the constitution of mixed gases; on the force of steam or vapour from water and other liquids in different temperatures, both in a Torricellian vacuum and in air; on evaporation; and on the expansion of gases by heat. Mem Lit Philos Soc Manchester 1802;5:536–602.
[25] Carrier WH. The Temperature of Evaporation ASHVE Trans 1918;24:25–50.
[26] ASHRAE. ASHRAE Handbook - HVAC Applications. 2007.
[27] Rohwer C. Evaporation from free water surfaces United States Department of. Agriculture 1931;No. 271.
[28] Smith CC, Löf G, Jones R. Measurement and analysis of evaporation from an inactive outdoor swimming pool. Sol Energy 1994;53. https://doi.org/10.1016/S0038-092X(94)90597-5.
[29] McMillan W. Heat dispersal—Lake trawsfynydd cooling studies. Symp Freshw Biol Electr Power Gener Part 1, Sess 1971;1:41–80.
[30] Sweers HE. A nomogram to estimate the heat-exchange coefficient at the air-water interface as a function of wind speed and temperature; a critical survey of some literature. J Hydrol 1976;30. https://doi.org/10.1016/0022-1694(76)90120-7.
[31] Richter D, Neubert W, Klämt A. Temperatur und Wärmehaushalt des thermisch belasteten Stechlin- und Nehmitzsees. Abh Meteor D d DDR 1979;16.
[32] ISO/TC 180/SC 4 N 140, Solar Energy - Heating Systems for Swimming Pools - Design and Installation. 1995.
[33] Klein SA. TRNSYS 17: A Transient System Simulation Program. Madison, USA: Sol Energy Lab Univ Wisconsin; 2010. p. 1.
[34] Li Y, Huang G, Xu T, Liu X, Wu H. Optimal design of PCM thermal storage tank and its application for winter available open-air swimming pool. Appl Energy 2018:209. https://doi.org/10.1016/j.apenergy.2017.10.095.
[35] Bergman TL, Lavine AS, Incropera FP, Dewitt DP. Fundamentals of heat and mass transfer, 2011. Fundamentals of Heat and Mass Transfer 2011.
[36] Shah MM. Improved method for calculating evaporation from indoor water pools. Energy Build 2012:49. https://doi.org/10.1016/j.enbuild.2012.02.026.
[37] Rakopoulos CD, Vazeos E. A model of the energy fluxes in a solar heated swimming pool and its experimental validation. Energy Convers Manag 1987:27. https://doi.org/10.1016/0196-8904(87)90075-6.
[38] Smith CC, Lof GOG, Jones RW. Rates of evaporation from swimming pools in active use. ASHRAE Trans 1998;104.
[39] Shah MM. New correlation for prediction of evaporation from occupied swimming pools. ASHRAE Trans 2013;119.
[40] Sartori E. Convection coefficient equations for forced air flow over flat surfaces. Sol Energy 2006:80. https://doi.org/10.1016/j.solener.2005.11.001.
[41] Duffie J, Beckman W. Solar Engineering of Thermal Processes. 2nd ed. USA: John Wiley and Sons. New York; 1991.
[42] J.H.E. Wattmuff a. Solar and wind induced external coefficient for solar collectors Coop Mediterr Pour l'Energue Solaire, Rev Int d'Heliotechnique 2nd Quart 1977.
[43] Australian Standards (3634 -1989). Solar Heating Systems for Swimming Pools. North Sydney, Australia.: 1989.
[44] Bowen IS. The ratio of heat losses by conduction and by evaporation from any water surface. Phys Rev 1926:27. https://doi.org/10.1103/PhysRev.27.779.
[45] Irmak S, Skaggs KE, Chatterjee S. A review of the Bowen ratio surface energy balance method for quantifying evapotranspiration and other energy fluxes. Trans ASABE 2014:57. https://doi.org/10.13031/trans.57.10686.
[46] Touma JS. Dependence of the wind profile power law on stability for various locations. J Air Pollut Control Assoc 1977:27. https://doi.org/10.1080/00022470.1977.10470503.
[47] Gliah O, Kruczek B, Etemad SG, Thibault J. The effective sky temperature: an enigmatic concept. Heat Mass Transf Und Stoffuebertragung 2011:47. https://doi.org/10.1007/s00231-011-0780-1.
[48] Evangelisti L, Guattari C, Asdrubali F. On the sky temperature models and their influence on buildings energy performance: a critical review. Energy Build 2019:183. https://doi.org/10.1016/j.enbuild.2018.11.037.
[49] Swinbank WC. Long-wave radiation from clear skies. Q J R Meteorol Soc 1963:89. https://doi.org/10.1002/qj.49708938105.
[50] Bliss RW. Atmospheric radiation near the surface of the ground: a summary for engineers. Sol Energy 1961:5. https://doi.org/10.1016/0038-092X(61)90053-6.
[51] Berdahl P, Martin M. Emissivity of clear skies. Sol Energy 1984:32. https://doi.org/10.1016/0038-092X(84)90144-0.
[52] Clark, G. Allen, C. The Estimation of Atmospheric Radiation for Clear and Cloudy Skies. Proc. 2nd Natl. Passiv. Sol. Conf., 1978, p. 675–8.
[53] G.N. Walton Thermal Analysis Research Program Reference Manual 1993 Natl Bur Stand.
[54] Jodat A, Moghiman M, Anbarsooz M. Experimental comparison of the ability of Dalton based and similarity theory correlations to predict water evaporation rate in different convection regimes. Heat Mass Transf Und Stoffuebertragung 2012:48. https://doi.org/10.1007/s00231-012-0984-z.
[55] İnan M, Özgür AŞ. Experimental Investigation of evaporation from a horizontal free water surface. Sigma J Eng Nat Sci 2017;35:118–31.
[56] Pauken MT. An experimental investigation of combined turbulent free and forced evaporation. Exp Therm Fluid Sci 1998:18. https://doi.org/10.1016/S0894-1777(98)10038-9.
[57] Marek R, Straub J. Analysis of the evaporation coefficient and the condensation coefficient of water. Int J Heat Mass Transf 2001:44. https://doi.org/10.1016/S0017-9310(00)00086-7.

[58] Tang R, Etzion Y. Comparative studies on the water evaporation rate from a wetted surface and that from a free water surface. Build Environ 2004:39. https://doi.org/10.1016/j.buildenv.2003.07.007.
[59] Guo Y, Cheng J, Liang S. Comprehensive assessment of parameterization methods for estimating clear-sky surface downward longwave radiation. Theor Appl Climatol 2019:135. https://doi.org/10.1007/s00704-018-2423-7.
[60] Carmona F, Rivas R, Caselles V. Estimation of daytime downward longwave radiation under clear and cloudy skies conditions over a sub-humid region. Theor Appl Climatol 2014:115. https://doi.org/10.1007/s00704-013-0891-3.
[61] Wu H, Tang R, Li Z, Zhong H. A mathematical procedure to estimate solar absorptance of shallow water ponds. Energy Convers Manag 2009:50. https://doi.org/10.1016/j.enconman.2009.03.005.
[62] Shah MM. Prediction of evaporation from occupied indoor swimming pools. Energy Build 2003:35. https://doi.org/10.1016/S0378-7788(02)00211-6.
[63] Meteonorm. Meteonorm - Global meteorological database 2012 Meteotest.
[64] Shah MM. Evaluation of methods for prediction of evaporation from water pools. J Build Phys 2022:45. https://doi.org/10.1177/17442591211034193.
[65] Waché R, Fielder T, Dickinson WEC, Hall JL, Adlington P, Sweeney SJ, et al. Selective light transmission as a leading innovation for solar swimming pool covers. Sol Energy 2020:207. https://doi.org/10.1016/j.solener.2020.06.022.
[66] Martin M, Berdahl P. Characteristics of infrared sky radiation in the United States. Sol Energy 1984:33. https://doi.org/10.1016/0038-092X(84)90162-2.
[67] Crawford TM, Duchon CE. An improved parameterization for estimating effective atmospheric emissivity for use in calculating daytime downwelling longwave radiation. J Appl Meteorol 1999;38. https://doi.org/10.1175/1520-0450(1999)038<0474:AIPFEE>2.0.CO;2.
[68] Gualtieri G. Improving investigation of wind turbine optimal site matching through the self-organizing maps. Energy Convers Manag 2017:143. https://doi.org/10.1016/j.enconman.2017.04.017.
[69] Nakajima K, Yamanaka T, Ooka R, Kikumoto H, Sugawara H. Observational assessment of applicability of Pasquill stability class in urban areas for detection of neutrally stratified wind profiles. J Wind Eng Ind Aerodyn 2020:206. https://doi.org/10.1016/j.jweia.2020.104337.
[70] Cook NJ. The Deaves and Harris ABL model applied to heterogeneous terrain. J Wind Eng Ind Aerodyn 1997:66. https://doi.org/10.1016/S0167-6105(97)00034-2.
[71] Irwin JS. A theoretical variation of the wind profile power-law exponent as a function of surface roughness and stability. Atmos Environ 1979:13. https://doi.org/10.1016/0004-6981(79)90260-9.
[72] Pasquill F. The estimation of the dispersion of windborne material. Meteor Mag 1961;90:33–49.
[73] Abubaker A, Kostić I, Kostić O. Numerical modelling of velocity profile parameters of the atmospheric boundary layer simulated in wind tunnels. IOP Conf. Ser Mater Sci Eng 2018;393. https://doi.org/10.1088/1757-899X/393/1/012025.